ENERGY MANAGEMENT IN WIRELESS SENSOR NETWORK OPERATIONS

A Dissertation

by

ARUPA KUMAR MOHAPATRA

Submitted to the Office of Graduate Studies of
Texas A&M University
in partial fulfillment of the requirements for the degree of

DOCTOR OF PHILOSOPHY

Chair of Committee,	Natarajan Gautam
Committee Members,	Georgia-Ann Klutke
	Kiavash Kianfar
	Richard Gibson
	Srinivas Shakkottai
Head of Department,	César Malavé

August 2013

Major Subject: Industrial Engineering

ABSTRACT

In this dissertation, we develop and analyze effective energy management policies for wireless sensor networks in emerging applications. Existing methods in this area have primarily focused on energy conservation through the use of various communication techniques. However, in most applications of wireless sensor networks, savings in energy come at the expense of several performance parameters. Therefore it is necessary to manage energy consumption while being conscious of its effects on performance. In most cases, such energy-performance issues are specific to the nature of the application. Our research has been motivated by new techniques and applications where efficient energy-performance trade-off decisions are required.

We primarily study the following trade-off cases: energy and node replacement costs (Case I), energy and delay (Case II), and energy and availability (Case III). We consider these trade-off situations separately in three distinct problem scenarios. In the first problem (Case I), we consider minimizing energy and node replacement costs in underwater wireless sensor networks for seismic monitoring application. In this case, we introduce mixed-integer programming (MIP) formulations based on a combined routing and node replacement policy approach and develop effective policies for large problem instances where our MIP models are intractable. In the second problem (Case II), we develop a Markov decision process (MDP) model to manage energy-delay trade-off in network coding which is a new energy-saving technique for wireless networks. Here we derive properties of the optimal policy and develop insights into other simple policies that are later shown to be efficient in particular situations. In the third problem (Case III), we consider an autonomous energy-harvesting sensor network where nodes are turned off from time to time to operate

in an "energy-neutral" manner. In this case, we use stochastic fluid-flow analysis to evaluate and analyze the availability of the sensor nodes under effective energy management policies.

In each of the above problem cases, we develop analytical formulations, and derive and/or analyze policies that effectively manage the considered energy-performance trade-off. Overall, our analyses and solution methods make new contributions to both operations research and communication networking literature.

DEDICATION

To Mom and Dad

ACKNOWLEDGEMENTS

I would like to express my sincere gratitude to my advisor Dr. Natarajan Gautam for providing me continuous guidance, support and encouragement during my years in the Ph.D. program. I would like to thank my committee members Dr. Georgia-Ann Klutke, Dr. Kiavash Kianfar, Dr. Richard Gibson and Dr. Srinivas Shakkottai for their valuable inputs in my research. I would also like to thank Dr. Guy Curry and Dr. Justin Yates for their academic advice and help on many occasions.

Many faculty and staff members in my department have helped me greatly on numerous occasions. I particularly thank Mrs. Judy Meeks for her help on administrative procedures. I wholeheartedly thank the department for providing me financial support through teaching assistantship during all these years. I also thank the Office of Graduate Studies for awarding me the Senator Phil Gramm Doctoral Fellowship which provided additional financial assistance.

Finally, I am grateful to my parents for their love and support. I also appreciate the help and encouragement from all my friends and colleagues.

TABLE OF CONTENTS

LIST OF FIGURES

LIST OF TABLES

TABLE Page

CHAPTER I

INTRODUCTION

Over the years, there has been a significant rise in the use of wireless sensor networks in industrial, environmental, military and other applications (see works by Akyildiz *et al.* [5] and Yick *et al.* [79] for an overview of main applications). Energy-efficiency in the operation of these networks is well-recognized as an important issue (Anastasi *et al.* [6]). This is primarily because these networks are often required to operate unattended for a long period of time with limited battery energy available to the sensors (also called nodes). The objective of this research is to develop and analyze effective policies for energy-efficient operation of such networks in emerging applications.

The energy consumption in a wireless sensor network can be managed in several ways depending on the nature of application. Since most of the energy of the sensors is used in wireless data transmission, energy savings are achieved by sending less data (using data aggregation and network coding techniques) or by scheduling and routing data transmissions in an efficient manner. These tasks are usually implemented through network communication protocols. However, in long-lived applications of wireless sensor networks (e.g. see seismic monitoring in Chapter II), energy conservation through any communication protocol is not sufficient to sustain network operation for the entire deployment period. In this case, in addition to operating the network with minimal energy, it is also required to replace the sensors when they run out of battery energy. Such node replacements may not be necessary in energy-harvesting sensor networks (see Chapter IV) which are now increasingly used in remote long-lived applications. But, in this case, the main constraint is

that the average energy generation rate of the sensors is less than their average energy consumption rate. Hence a resource allocation policy is required here to efficiently balance energy consumption against the amount of energy generated. This is commonly done by "sleep-scheduling" where sensors are switched off time to time according to a policy or schedule.

Based on the nature of application, one or more of the above approaches (i.e. communication protocol, node replacement and resource allocation) are used for managing energy in wireless sensor networks. Though energy-efficient communication methods have received a lot of attention in the literature, there is very limited work on node replacement and resource allocation policies for managing energy in sensor networks. Further, the majority of existing methods aim either to minimize the energy consumption in the network or to maximize the network life. But in most applications of wireless sensor networks, savings in energy usually come at the expense of various performance parameters. Therefore it is necessary to make effective decisions to optimize energy consumption as well as performance. Though certain energy-performance trade-off issues (e.g. energy-delay trade-off) have been studied in specific contexts, new application scenarios warrant entirely different analyses. Also, there is a need to develop decision models for other important trade-off cases.

In this research, we focus on developing effective energy management policies for important applications of wireless sensor networks. Our work has been motivated by new techniques and applications where specific energy-performance trade-off decisions are required. We are primarily interested in studying the following trade-off cases.

- **Energy and delay:** In certain techniques for wireless networks, energy consumption is reduced by accumulating data for more energy-efficient transmis-

sions in future. However, the achieved energy savings may be offset by the delays in transmissions. Hence it is required to have a decision model to efficiently trade-off between low energy consumption and high quality-of-service (i.e. low delay).

- **Energy and availability:** In common resource allocation approaches for energy management in sensor networks, nodes are switched off for certain periods to conserve energy. Note that, the availability (i.e. proportion of the time for which the network is operational or available with respect to the total time) of the network decreases with an increase in the number of sensors that are off. Therefore the resource allocation policy must try to manage the energy consumption of the sensors in such a way that availability is maximized.

- **Energy and node replacement costs:** Recall that, in long-lived applications of wireless sensor network with battery-powered nodes, it is necessary to replace the energy-depleted nodes to ensure continuous operation. In multihop wireless sensor networks, energy consumption and node replacement costs have an interesting interdependence. Note that the node replacement cost includes both cost of energy (in a new node) and the cost of labor. When a single sensor node is considered, energy conservation will lead to less number of replacements of the node, and therefore node replacement costs are reduced. However, in case of a sensor network, the sensor nodes usually consume energy at different rates (which depend on the routing strategy), and hence they require replacement at different times. In this case, when the node replacement cost structure has a high fixed cost involved, replacing several nodes together may be cost-effective. This may include preventive replacement of some nodes that still have some unused energy. Therefore, though it is essential to conserve

energy to minimize the node replacement costs, preventive node replacement (which wastes unused energy) should also be used to an optimal degree.

In this dissertation, we consider the above trade-off cases separately in three distinct problem scenarios. We summarize these problem scenarios in Table 1. In the first problem (Case I), we develop effective methods to manage energy and node replacement costs in underwater wireless sensor networks for seismic monitoring application. In this case, we devise a combined routing and node replacement policy approach which is new to the literature. In the second problem (Case II), we consider energy-delay trade-off issues in network coding which is a new energy-saving technique for wireless networks. Here we develop effective policies to manage the energy-delay trade-off in a mobile/ad-hoc wireless sensor network setting. In the third problem (Case III), we consider an autonomous energy-harvesting sensor network where nodes are turned off time to time to operate in an "energy-neutral" manner. In this case, we evaluate and analyze the availability of the sensor nodes under effective energy management policies. Note that though it may be possible to analyze a combination of all the above scenarios, it is hard to envision a practical

Table 1: Considered problem cases

Case	**I (Chapter II)**	**II (Chapter III)**	**III (Chapter IV)**
Considered trade-off	energy and node replacement costs	energy and delay	energy and availability
Considered application	seismic monitoring using underwater wireless sensor network	mobile/ad-hoc wireless sensor network	wireless sensor network with energy-harvesting nodes
Energy conservation approach	routing	network coding	node activation policy
Energy replenishment approach	node replacement	–	recharge process

application that would justify such an analysis.

Our common objective in all these problems is to develop and/or analyze policies to manage energy consumption while minimizing the adverse effects on other performance parameters. In problem cases I and II, we develop optimization models to characterize the optimal policy, study their useful properties and develop tractable solution methods. In problem case III, our objective is to develop analytical models to evaluate performance under given policies. Given the diverse nature of the considered problems and applications, we have presented the related literature review and problem challenges separately in forthcoming sections.

The remainder of this dissertation is organized as follows. We present the considered problem cases I, II and III in Chapters II, III and IV respectively. Each of these chapters provides discussions on problem background, literature review, problem formulation, solution methods and numerical results. Finally, in Chapter V, we outline important contributions of this research and present our concluding remarks.

CHAPTER II

CASE I: MANAGING ENERGY AND NODE REPLACEMENT COSTS IN UNDERWATER WIRELESS SENSOR NETWORKS FOR SEISMIC MONITORING*

II.1 Introduction

Over the last several years, there has been a significant rise in interest in underwater wireless sensor networks for a wide range of applications (e.g. seismic monitoring of undersea oilfields (Heidemann *et al.* [24], Li *et al.* [46]), marine environment monitoring (Akyildiz *et al.* [4], Vasilescu *et al.* [76]) and offshore surveillance (Akyildiz *et al.* [4], Pompili and Melodia [55])). As underwater sensor networks have begun to be deployed in many applications, cost-efficiency in the operation of these networks has now become an important issue. Unlike most terrestrial sensor networks, underwater sensors (also called nodes here) are very expensive and are deployed for prolonged (nearly permanent) monitoring operation. Also, to ensure continuous operation, it is necessary to replace these nodes when they run out of battery energy. However, given the remote offshore location of the network, the node replacement costs are very high and are a major component of the total operating cost. In this chapter, we develop effective policies to minimize this cost in the seismic monitoring application.

II.1.1 Seismic Monitoring

Our main motivation comes from the need to use underwater wireless sensor networks in the petroleum industry which is heavily dependent on seismic methods to

find various changes in oil and gas reservoirs as responses to production. Ocean bottom seismic systems are emerging as superior information-acquisition methods in seismic monitoring of undersea oilfields. These systems use a large network of sensor nodes (known as ocean bottom seismometers (OBS)) that are laid on the ocean floor to collectively gather and transmit seismic information. At present, a majority of OBS acquisition methods use a wired underwater node network (known as ocean bottom cable (OBC) method (Seymour and Barr [66])) wherein nodes are connected by fiber-optic cables on the ocean floor. However, in this method, installation and operating costs are extremely high. Further, deploying miles of heavy cable and sensor packages on the ocean floor causes substantial damage to the marine environment. Hence as an alternative, some applications have started using autonomous data-storage nodes which are required to be retrieved regularly to collect the data stored in them (SeaBed Geophysical [61]). However, unlike the cable-based acquisition, the inability of this method to retrieve seismic data in real-time is a major limitation. In fact there is an increasing need for real-time seismic information in the oil industry to improve reservoir management and optimize production. Thus the idea of using nodes with wireless data transmission capability has recently gained interest in this application (Heidemann *et al.* [24]). This method retains all major benefits of autonomous nodes and provides opportunity for real-time monitoring.

We consider OBS acquisition by a suitable underwater wireless sensor network. We mainly focus on the use of this network for passive seismic monitoring (also known as microseismic monitoring) application where all nodes continuously monitor signals from microseismic activities in the undersea reservoir. The ability of passive seismic method to monitor dynamic processes in real time has led to its increasing use in recent years (Duncan [19], Martakis *et al.* [49], Maxwell and Urbancic [50]). The underwater passive seismic network can also be used to conduct conventional

active seismic surveys to monitor reservoir fluid movements at intervals on the order of several months to a year. In active seismic data acquisition, "air gun" sources generate acoustic waves by injecting compressed air into the seawater. These waves propagate into the earth and the nodes on the seabed (in OBS acquisition) measure the velocity and pressure of the waves reflected from different undersea rock layers. Here the collected data is primarily used to produce a 3D or 4D (time lapse) seismic image of the undersea oilfield.

In an underwater passive seismic network, all nodes continuously sense and transmit information to data-gathering sink nodes via multi-hop wireless transfer. However, as the battery energy available to the nodes is limited, the deployment period (usually 20-50 years) of the network extends well beyond the lifetimes of the nodes. Hence nodes must be replaced on or before complete energy loss to ensure continuous monitoring from all node locations. We aim to minimize these node replacement costs which are very high over the deployment period. To achieve this, we employ a combined routing and node replacement policy approach which we describe next.

II.1.2 Combined Routing and Node Replacement Policy

The node replacement operation in underwater seismic node networks involves a fixed setup cost per replacement attempt and an additional cost per individual node replacement. The fixed setup cost primarily involves sending a crew and equipment to the remote off-shore location. This implies that costs can be saved by replacing several nodes together at a time. Note that, in case of an extremely high fixed cost, it would be optimal to replace all the nodes in the network when a replacement attempt is made. On the other hand, when this fixed cost component is reasonably low, only replacing nodes as they fail would be cost-effective. In our application, the fixed setup cost is certainly very high, but the variable cost component for individual node

replacement is not negligible either. Hence there is a need for developing an effective replacement policy to minimize the replacement costs. This node replacement policy (or schedule) will specify when to make replacement attempts and which nodes to replace in every single attempt. However, node replacement decisions alone do not control the replacement costs. Note that the average rate of replacement of every node depends on its energy consumption rate which is primarily dependent on the amount of data transmission handled by the node. Since the data generation rate is fixed at all the nodes, transmission loads are mainly decided by the routing strategy that specifies the distribution of packet transmissions on different routes from each node. Thus the routing method not only needs to be energy-efficient, but it must also work well with the replacement policy to minimize the replacement costs. Hence the node replacement costs can be effectively controlled by a combined policy of routing and node replacement decisions.

Most of the known routing and node replacement techniques developed for terrestrial sensor networks are not suitable for our considered seismic monitoring application. The main challenges for routing and node replacement in underwater seismic node networks are: (1) high energy consumption in acoustic transmission, (2) continuous energy consumption by the nodes, and (3) high cost of the node replacement combined with the economies of scale in the replacement cost structure. Due to these challenges and specific requirements, we develop new strategies for routing and node replacement in underwater seismic networks.

The remainder of this chapter is organized as follows. We present a review of related works in Section II.2. In Section II.3, we provide combined routing and node replacement formulations to minimize node replacement costs in a generic sensor network. Section II.4 outlines the network model and assumptions specific to the seismic monitoring application. In Section II.5, we develop effective methods to minimize

node replacement costs in our considered seismic node network. We report our computational results in Section II.6. Finally, in Section II.7, we present our concluding remarks and some future research directions in the domain of this problem.

II.2 Literature Review

Both routing and replacement problems have received a lot of attention in the literature, but they have mostly been addressed independent of each other. In particular, many energy-efficient routing algorithms are available for both terrestrial and underwater networks. The majority of these routing algorithms, mostly available for terrestrial sensor networks, can be divided into two main categories. Various routing techniques in the first category try to minimize the overall energy consumption in the network (Heinzelman *et al.* [27], Singh *et al.* [69]). The routings in the second category try to maximize network use by balancing energy consumption throughout the network (Chang and Tassiulas [16], Shah and Rabaey [67]). Further, recent energy-aware routing approaches by Lin *et al.* [47] and Zeng *et al.* [80] consider nodes with renewable energy sources that can replenish energy at a certain rate. For long-lived network applications like seismic monitoring, replacement of nodes is unavoidable since energy conservation through routing (or any other communication protocol) is not sufficient to sustain network operation for the entire deployment period. Hence node replacement in wireless sensor networks has received significant attention recently. Tong *et al.* [74] developed a node replacement policy as well as an algorithm to schedule the replacement of individual nodes in a replacement attempt. Parikh *et al.* [54] developed several node replacement policies to maintain a threshold sensing coverage in wireless sensor networks.

There are various replacement models available in the operations research literature on maintenance of multicomponent systems such as our node network. Kobbacy

et al. [40] provide a comprehensive review of multicomponent maintenance models developed before 2006. In particular, Assaf and Shanthikumar [9], Dekker and Roelvink [18], Ritchken and Wilson [59], Wilson and Benmerzouga [77], and Zheng [81] have developed various important results related to group replacement policies for multicomponent systems. Most of these models consider a distribution function for deterioration of the components. The continuous energy loss of the nodes in our problem is equivalent of such a deterioration process. As the number of states of the system rise exponentially with the number of components, finding an optimal replacement policy for such a system with sizable number of components is computationally infeasible (Kobbacy *et al.* [40]). Recent works by Heidergott [25], Heidergott and Farenhorst-Yuan [26], and L'Ecuyer *et al.* [45] have focused on age replacement policies due to their simplicity and effectiveness. These are state-independent policies where components are replaced when they attain a certain age threshold (equivalently a residual energy threshold for our nodes). The "FRP" and "FRD" policies that we introduce in Section II.5 are indeed threshold-based replacement policies.

II.3 Combined Routing and Node Replacement in a Generic Sensor Network

In this section, we provide mathematical formulations for minimizing node replacement costs in a generic sensor network. We will consider the special case for seismic monitoring application in Section II.4 onwards.

Consider a network of N similar nodes that will be utilized over a long time period, say T days. Let the data-gathering sink node be denoted as the $(N+1)$-st node. In every data collection *round*, node-i ($i = 1, \ldots, N$) generates s_i number of packets and sends them to the sink node via multihop routing. Assume that there are D rounds of data collection in a day. Let U_i be the set of nodes from which

node-i can directly receive data, and let V_i be the set of nodes to which node-i can directly transmit. Node-i consumes E_{ij}^T amount of energy to transmit a packet to node-j ($j \in V_i$). Additionally every node consumes E^R amount of energy to receive a packet. The initial amount of energy stored in a new node is E_0. Recall that the nodes must be replaced on or before complete energy loss. Let K be the setup cost of a replacement attempt and C be the cost of replacing a node.

Our objective is to achieve the minimum average node replacement cost in the network by joint control of routing and node replacement policies. The routing decision specifies how every node will distribute its packet transmissions to all nodes within its range. The node replacement policy or schedule specifies when to make a replacement attempt and which nodes to replace in an attempt. To reduce the problem size and increase convenience in network operation, we assume that routing and node replacement decisions are made at the beginning of every day in the time horizon instead of every data collection round.

It is not possible to develop a tractable mathematical formulation for our problem in the given setup. Hence we modified the problem slightly and obtained an equivalent mixed integer programming (MIP) formulation (Wolsey [78]) that we subsequently prove optimal for the original problem. In the modified setup, we can replace an energy-depleted node with a new node with any amount of battery energy up to E_0. However, the cost of replacing the node is kept the same irrespective of the amount of energy stored in the new node. Note that, in the original setup of our problem, the new replacement nodes have full battery energy E_0. Now we define our decision variables below.

r_{ij}^t = number of packets sent in every round from node-i to node-j in day-t,

$x^t = 1$ if a node replacement attempt is made on day-t, else 0,

$y_i^t = 1$ if node-i is replaced on day-t, else 0.

Additionally, let e_i^t denote the amount of energy remaining in node-i at the beginning of day-t (just before a possible replacement). Note that it only makes sense to replace a node with a new node with a higher amount of energy. If node-i is replaced on day-t, let w_i^t be the additional amount of energy in the incoming new node over the outgoing node (i.e. the energy stored in the new node is $e_i^t + w_i^t$). Now, in the modified setup, the optimal routing and node-replacement decisions minimizing the total replacement cost (or equivalently minimizing the replacement cost per day) can be obtained from the solution to the following MIP problem.

(MIP-1):

$$\text{Min} \quad f_1(\boldsymbol{r}, \boldsymbol{x}, \boldsymbol{y}) = K \sum_{t=1}^{T} x^t + C \sum_{t=1}^{T} \sum_{i=1}^{N} y_i^t \tag{1}$$

$$\text{s.t.} \quad \sum_{j \in V_i} r_{ij}^t - \sum_{j \in U_i} r_{ji}^t = s_i, \qquad i = 1, \ldots, N,\ t = 1, \ldots, T \tag{2}$$

$$\sum_{j \in U_{N+1}} r_{j,N+1}^t = \sum_{i=1}^{N} s_i, \qquad t = 1, \ldots, T \tag{3}$$

$$e_i^1 = E_0, \qquad i = 1, \ldots, N \tag{4}$$

$$e_i^{t+1} = e_i^t + w_i^t - D \left(\sum_{j \in V_i} E_{ij}^T\, r_{ij}^t + E^R \sum_{j \in U_i} r_{ji}^t \right), \qquad i = 1, \ldots, N,\ t = 1, \ldots, T \tag{5}$$

$$e_i^t + w_i^t \leq E_0, \qquad i = 1, \ldots, N,\ t = 1, \ldots, T \tag{6}$$

$$w_i^t \leq E_0\, y_i^t, \qquad i = 1, \ldots, N,\ t = 1, \ldots, T \tag{7}$$

$$y_i^t \leq x^t, \qquad i = 1, \ldots, N,\ t = 1, \ldots, T \tag{8}$$

$$r_{ij}^t \geq 0, \qquad i = 1, \ldots, N,\ j \in V_i,\ t = 1, \ldots, T \tag{9}$$

$$e_i^t \geq 0, \qquad i = 1, \ldots, N,\ t = 1, \ldots, T+1 \tag{10}$$

$$w_i^t \geq 0,\ x^t \in \{0, 1\},\ y_i^t \in \{0, 1\}, \qquad i = 1, \ldots, N,\ t = 1, \ldots, T. \tag{11}$$

In the above formulation, the objective function (1) aims to minimize the total node replacement cost over the time horizon. In (2)-(3), we present the packet balance conditions which must hold for any routing in the network. Equation (4) indicates that network operation is started with nodes with full battery energy. In (5), we provide energy-balance conditions for each node at the beginning of each day. As per (6), the incoming new node can have stored energy up to the limit E_0. Inequality (7) stipulates the condition that the additional energy of a new replacement node can be considered only if a node replacement decision is made. As per (8), replacement of a node is possible only if a replacement attempt is made. Equations (9)-(11) specify the nature of the decision variables.

In the following proposition, we show that the solution to MIP-1 is actually the solution to our node replacement cost minimization problem in the original setup (i.e. where all new replacement nodes have full battery energy E_0).

Proposition 1. *The optimal routing and node replacement decisions in MIP-1 (modified setup) are also optimal in minimizing the node replacement costs in the original setup.*

Proof. Let z^* and z^{**} be the optimal total node replacement costs in MIP-1 (modified setup) and in our original problem respectively. In our original setup, new replacement nodes have full battery energy, i.e. $e_i^t + w_i^t = E_0$ whenever $y_i^t = 1$. Note that such node replacement options are also considered in the formulation MIP-1 (see (6)). In fact MIP-1 minimizes the total node replacement cost over a broader set of node replacement options than our original problem. In other words, MIP-1 is a relaxed formulation of our original problem. Hence, we have $z^* \leq z^{**}$.

Now consider the optimal solution $\{{r_{ij}^t}^*, x^{t*}, y_i^{t*}, w_i^{t*}, e_i^{t*}\}$ of MIP-1. Since replacing with a new node with any amount of energy up to E_0 costs the same amount C,

we can construct an alternate optimal solution of MIP-1 (with the same objective value z^*) as $\{r_{ij}^{t\,*}, x^{t*}, y_i^{t*}, w_i^{t**}, e_i^{t**}\}$, where $w_i^{t**} + e_i^{t**} = E_0$ whenever $y_i^{t*} = 1$ and the relation $e_i^{t+1**} = e_i^{t**} + w_i^{t**} - D\Big(\sum_{j\in V_i} E_{ij}^T\, r_{ij}^{t\,*} + E^R \sum_{j\in U_i} r_{ji}^{t\,*}\Big)$ is recursively satisfied. However, since all the new replacement nodes have full battery energy in this solution, the decision $\{r_{ij}^{t\,*}, x^{t*}, y_i^{t*}\}$ is actually a feasible solution to our original problem. Therefore we have $z^* \geq z^{**}$.

Based on the above arguments, we have $z^{**} = z^*$, and $\{r_{ij}^{t\,*}\}$ and $\{x^{t*}, y_i^{t*}\}$ are the optimal routing and node replacement decisions for our original problem. □

When a fixed routing decision over the entire time horizon (i.e. $r_{ij}^t = r_{ij}$ for all t) is intended in the solution of MIP-1, only one set of routing constraints (see (2)-(3)) will suffice for all values of t. We will refer to this fixed routing version (of MIP-1) as MIP-2. When a preselected fixed routing $\{r_{ij}\}$ is used in the network, the optimal node replacement schedule can be found by solving a reduced version of MIP-1 where the routing constraints given by (2)-(3) are removed. However, this particular problem can be more efficiently solved in the original setup. In this case, the lifespan (in days) of node-i is estimated as $L_i = \Big\lfloor E_0 / \Big(D\Big\{\sum_{j\in V_i} E_{ij}^T\, r_{ij} + E^R \sum_{j\in U_i} r_{ji}\Big\}\Big)\Big\rfloor$. Now the node replacement schedule minimizing the total replacement cost (or equivalently minimizing the replacement cost per day) can be obtained from the solution to the following integer programming (IP) problem.

$$\text{(IP-3):}\ \text{Min} \quad f_3(\boldsymbol{x}, \boldsymbol{y}) = K\sum_{t=2}^{T} x^t + C\sum_{t=2}^{T}\sum_{i=1}^{N} y_i^t \tag{12}$$

$$\text{s.t.} \quad y_i^t \leq x^t, \qquad i = 1,\ldots,N,\ t = 1,\ldots,T \tag{13}$$

$$y_i^1 = 1, \qquad i = 1,\ldots,N \tag{14}$$

$$\sum_{t=k}^{k+L_i-1} y_i^t \geq 1, \qquad i = 1,\ldots,N,\ k = 1,\ldots,(T - L_i + 1) \tag{15}$$

$$x^t, y_i^t \in \{0,1\}, \qquad i = 1,\ldots,N,\ t = 1,\ldots,T, \tag{16}$$

where x^t and y_i^t are node replacement decisions at the beginning of a day for a replacement attempt and an individual node replacement respectively. Inequality (13) specifies that a node can be replaced only when a replacement attempt is made. Equation (14) indicates that network operation is started with nodes with full battery energy. However, note that using new nodes at beginning is not actually node replacement and hence its cost is ignored in the objective function (12). As per (15), the i-th node must be replaced at least once in any span of L_i days. This ensures that every node is replaced on or before complete energy loss.

Our combined routing and node replacement formulation MIP-1 as well as its simpler variant MIP-2 are intractable for a network with large number of nodes (N) and for a long deployment period (T). The difficulty is mainly due to large number of binary decision variables and the constraints given by (7) and (8) in particular. The formulation IP-3 is also hard to solve for sizable problem instances. Therefore, to minimize the node replacement costs in the considered seismic node network, we need to develop methods that are effective and suitable for practical implementation.

II.4 Seismic Network Model and Assumptions

In this section, we explain the structure of the underwater sensor network that we have considered in our model for seismic monitoring application. We also present important assumptions that are used in subsequent sections.

The area of the ocean floor covering a petroleum reservoir ranges between 50-100 km^2. In ocean bottom seismic acquisition, nodes (i.e. underwater sensors) are deployed over this area usually in a square or rectangular grid (Heidemann *et al.* [24]). For passive seismic application, the inter-node distance on this grid varies from a few hundred meters to 1 km. Recall that the seismic data from all the nodes must be available for analysis in real time. Hence all data from the nodes are sent

to one or more sink nodes via muitihop wireless transmission. The sink node can be connected via a high-speed optical link to a node floating on the sea surface, and the latter can forward the received information to the base station via a radio link. Since the size of the seismic node network and its coverage area are very large, the whole network is divided into smaller independent networks with a separate sink node for each individual network (Heidemann *et al.* [24]). All our analyses in this chapter are based on one such independent network of 120 nodes that are positioned on a square grid. Figure 1 shows the structure of this network along with two routing strategies that we will discuss in Section II.5.

Observe (in Figure 1) that the nodes in our network can be thought of as being arranged in concentric squares around the sink node, and nodes on a particular square can be identified by a level. In our convention, the closer the square is to the center, the lower is its level. We assume that a node in a particular level can send data to nodes within its transmission range in the next lower level. Given the noisy underwater environment and the long distance of separation between nodes, such one-hop transmission is a reliable option. For every node to have at least one other node within its range, we set the transmission range of every node at $\sqrt{2}d$ for an inter-node distance d on the grid.

Now we will briefly describe how our model and assumptions meet acoustic transmission requirements. Considering 24 bits per component in a standard 4-component seismic acquisition (with three geophones and one hydrophone in each node) with a 50 ms sampling rate, and allowing some overhead, every node generates a 2000-bit packet every second. Then it transmits its own packet and other forwarded packets to one or more nodes within its transmission range. It can be observed in the forthcoming Section II.5 that using uniform nodes with 50 kbps output capacity will safely ensure congestion-free continuous transmission with our proposed routing schemes.

Note that 50 kbps acoustic transmission is possible with an appropriate frequency over our selected inter-node distances (Kilfoyle and Baggeroer [39]).

We will now provide mathematical expressions to calculate energy consumption at the nodes. Since most of the energy of a node is consumed in the underwater acoustic data transmission, energy consumed in sensing is negligible, and we have ignored it in our model. Energy consumption in acoustic transmission depends on both distance (d) and frequency (f) of transmission. In our energy consumption model, we have adapted the calculations to the radio transmission case (Heinzelman *et al.* [27], Kalpakis *et al.* [31]). In our model, energy consumed (in J/bit) at a node per bit of data transfer is given by

$$\text{(For sending)} \quad E_T(f,d) = E_{\text{elec}} + \frac{P_T(f,d)}{B}, \tag{17}$$

$$\text{(For receiving)} \quad E_R = E_{\text{elec}}, \tag{18}$$

where $E_T(f,d)$ is the amount of energy to transmit 1 bit of data over a distance of d at frequency f in terms of $E_{\text{elec}}, P_T(f,d)$ and B which we define next. In (17), the fixed component E_{elec} [J/bit] is the energy consumed by the electronic circuitry and $P_T(f,d)$ [W] is the power at which the transmitter operates specific to the frequency and the distance of transmission. The output capacity of a node for the acoustic transmission is B bits/sec. By (18), a node will consume E_R amount of energy for receiving 1 bit of information. We have assumed a nominal value of 50 nJ/bit for E_{elec}. We have set the frequency (f) at 75 kHz for all transmissions. We earlier explained our choice of 50 kbps for B. We derive an expression to compute $P_T(f,d)$ in Appendix A.

Having described the network structure and the data transmission model, now we will consider certain costs for our model. Recall from Section II.1 that the nodes

are to be replaced when they run out of battery energy. However, the sink node is externally powered and hence will not need replacement. Node replacement implies that a new battery must be provided, but in the harsh deep water environment, it is most practical to replace the entire node. In this case, the node can be reused later with a new battery. We assume that the total cost in a replacement attempt is of the form $K + Cx$, where K is the fixed set-up cost of a replacement attempt, C is the cost of replacing a node and x is the number of nodes replaced in an attempt. The parameter C includes the cost of a new battery and cost for labor time in an individual node replacement.

II.5 Routing and Node Replacement Policies for a Seismic Node Network

In this section, we develop effective methods to minimize the average maintenance (for node replacement) cost in a passive seismic node network. Recall from Section II.1 that, in a passive seismic network, all nodes continuously monitor the microseismic events and send the recorded information periodically to the sink node via multi-hop wireless transfer. For this application, we consider a 120-node grid-structured network (see Figure 1(a)) with an inter-node distance of 200 m.

Given the size of the considered network and its long period of operation (20-50 years), it is not possible to solve its MIP-1 formulation to attain the optimal average node replacement cost. Also note that the formulations MIP-2 (for fixed routing decision) and IP-3 (with a given fixed routing) are hard to solve in this case. Hence we will now develop new techniques taking advantage of the special structure of the seismic node network. We know that the node replacement costs can be effectively controlled by both routing and node replacement decisions. Based on this idea, in the following subsections, we introduce efficient routing and node replacement policies

and use them in combinations to minimize the average maintenance cost of the network. To maintain consistency with Section II.3, routing and node replacement decisions are considered on a per day basis instead of per round.

II.5.1 Routing

As we have mentioned in Section II.2, routing in sensor networks has been well-studied. However, given the focus on minimizing the node replacement costs in our application, we investigate new strategies for routing packets in the network. Our aim is to minimize the number of replacement attempts as well as the total number of nodes replaced in all attempts. Hence a suitable routing scheme must have two major characteristics. First, it should have groups of large number of nodes having closest possible energy dissipation rates so that the nodes in these groups can be replaced at the same time. This will ensure a smaller number of replacement attempts. Secondly the routing should be energy-efficient to minimize the total number of node replacements. For our grid network, the minimum energy (also called minimum total energy (MTE) (Chang and Tassiulas [16])) routing schemes that are symmetric about the center best satisfy these two requirements. These routings minimize the total energy consumed in all transmissions in a data collection round (which, in our case, leads to the receipt of 120 packets at the sink node and repeats every second).

In our grid network case, there are multiple minimum energy routing solutions available. From these solutions, considering symmetry around the center, we selected ME-1 (Figure 1(a)) and ME-2 (Figure 1(b)) routings which we describe next. In the ME-1 routing scheme, every node sends all its packets to the nearest node in its next lower level. Similarly in the ME-2 routing, most of the nodes send all their packets to the farthest node in the next lower level. The number of packets sent per round from

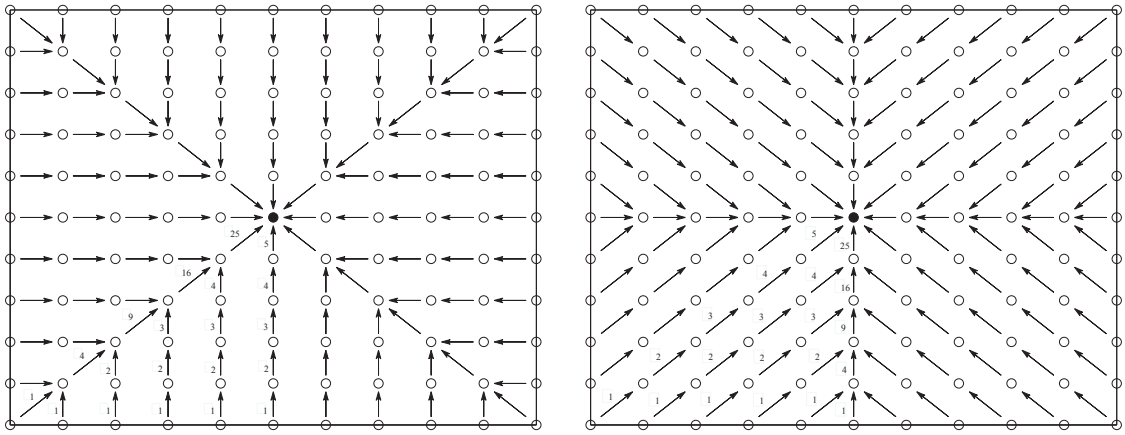

(a) ME-1 (b) ME-2

Figure 1: Selected minimum energy routings in grid network

each node in the network is shown in Figure 1 for both routings. In the following proposition, we present an important difference between ME-1 and ME-2 routings.

Proposition 2. *When most nodes in the network have sufficient energy, ME-2 routing sustains network operation for a longer period of time than ME-1 routing until a node requires replacement.*

Proof. Suppose u_i^1 and u_i^2 are energy consumption rates of the i-th node ($i = 1, \ldots, N$) in ME-1 and ME-2 routings respectively. Also, let E_i be the amount of energy remaining in node-i at a particular time. From this point, the time until next node replacement in case of ME-1 and ME-2 routings will be $T_1 := \min_i \lfloor E_i/u_i^1 \rfloor$ and $T_2 := \min_i \lfloor E_i/u_i^2 \rfloor$ respectively.

We can see (in Figure 1) that the number of packet transmissions increases towards the center both in case of ME-1 and ME-2 routings. Hence the nodes close to the center consume energy at a faster rate than the nodes far from the center. However, an increasingly large number of packets are sent over the diagonal inter-node distance ($\sqrt{2}d$) in ME-1 routing whereas this happens over the lateral inter-node

distance (d) in ME-2 routing. Hence we have $\max_i u_i^1 > \max_i u_i^2$. Therefore, when E_i's are sufficient, we have $T_1 < T_2$. □

Now, by running a combination of ME-1 and ME-2 routings (while keeping the total energy consumption in a round still minimum), we can increase the network survivability further. For such a hybrid routing which we will call ME-H, the optimal combination of ME-1 and ME-2 routings can be found from the solution to the following integer programming problem.

$$\text{(IP-4):}\quad \text{Max} \quad X_1 + X_2 \tag{19}$$

$$\text{s.t.} \quad u_i^1 X_1 + u_i^2 X_2 \leq E_i, \qquad i = 1, \ldots, N \tag{20}$$

$$X_1, X_2 \geq 0, \text{integer}, \tag{21}$$

where u_i^1 and u_i^2 are the per-day energy consumption rates of node-i in ME-1 and ME-2 routings respectively, E_i is the amount of energy in node-i at the time of consideration, and X_1 and X_2 are the number of days for which the ME-1 and ME-2 routings will be run respectively. We will use these energy-efficient ME-1, ME-2 and ME-H routings for all our models in subsequent sections.

II.5.2 Node Replacement Policy

A node replacement policy for our problem is a rule to decide when to make a replacement attempt and which nodes to replace in an attempt. Recall from Section II.1 that the economies of scale in the replacement cost model lead to cost savings when several nodes are replaced during a replacement attempt. So, while replacing the completely energy-exhausted nodes, it will be cost-effective to replace some additional nodes that have low residual energy. Hence a node replacement policy for our problem will essentially try to use this preventive replacement option

to an optimal degree to minimize the average maintenance cost.

Note that the formulations MIP-1, MIP-2 and IP-3 do allow preventive node replacement when it is optimal to do so. However, besides the known intractability of these formulations for sizable problem instances, the possible optimal replacement schedules in these cases may be highly irregular and hence are not suitable for practical implementation. In fact we require replacement policies to be fixed, simple and easy to implement. Based on these considerations, we propose the following three replacement policies to decide when to make replacement attempts and which nodes to replace in every attempt.

1. *Fixed Interval Replacement (FI):* Here the time interval between replacement attempts is fixed. If we fix this interval as F days, a replacement attempt can be made on days numbered kF (for $k = 1, 2, \ldots$). On any replacement attempt, all nodes that will not survive until the next possible attempt will be replaced. Also, a replacement attempt will not be made if all nodes are known to survive until the next possible attempt.

2. *Fixed Residual Energy - Percentage-based Replacement (FRP):* With this policy, a replacement attempt is made only when a node fails, and all nodes with residual energy less than a fixed threshold level are replaced. Here we specify this energy threshold as a percentage ($p\%$) of initial battery energy E_0.

3. *Fixed Residual Energy - Day-based Replacement (FRD):* This policy is similar to FRP. In this case, a replacement attempt is made only when a node fails, and all nodes with residual energy not sufficient to survive for at least another F_{FRD} (fixed) number of days are replaced. Note that the residual energy threshold here is the amount of energy just sufficient for F_{FRD} number of days.

In each of above policies, either the decision for a replacement attempt or the decision on individual node replacement is based on a simple fixed strategy. Note that both FRP and FRD are threshold-based replacement policies. However, unlike FRP, the residual energy threshold levels in FRD are different for nodes with different energy consumption rates. Also, the main difference between FI and FRD replacement policies is in the decision about when to make a replacement attempt.

II.5.3 Combining Routing and Node Replacement Policies

Now we will describe how our proposed replacement policies (FI, FRP and FRD) can be used with ME-1, ME-2 and ME-H routings. It can be observed from the definitions of FI, FRP and FRD policies that they are easily implementable with a fixed routing such as ME-1 and ME-2. Note that, when a fixed routing is used, any replacement schedule over a time period of T days is a feasible solution to the problem IP-3. Hence for ME-1 and ME-2 routings, the replacement schedules given by FI, FRP or FRD policies will not be any better than the IP-3 solution schedule. However, we seek to answer the question how good they are. In fact these schedules, unlike the IP-3 solution, are easy to find, and they always have some regularity associated with them.

The ME-H routing is easy to use only with the FRP replacement policy. When it is used with the FI or FRD policy, it is not clear which nodes to replace in a replacement attempt. This is because X_1 and X_2 values (following a replacement) are not known at the time of replacement, and hence the knowledge of whether a node will last for additional F (F_{FRD} for FRD policy) number of days is not available at that time. Recall that X_1 and X_2 are the number of days for which the ME-1 and ME-2 routings will be run respectively. We propose the following integer programming model that helps decide which nodes to replace in a replacement attempt in case of

ME-H routing with FI policy (use F_{FRD} in place of F for FRD policy):

$$\text{(IP-5):}\ \text{Min} \quad f_5(\boldsymbol{y}) = \sum_{i=1}^{N} y_i \tag{22}$$

$$\text{s.t.} \quad u_i^1 X_1 + u_i^2 X_2 \leq E_i(1 - y_i) + E_0\, y_i, \quad i = 1, \ldots, N \tag{23}$$

$$X_1 + X_2 \geq F \tag{24}$$

$$X_1, X_2 \geq 0, \text{integer} \tag{25}$$

$$y_i \in \{0, 1\}, \qquad i = 1, \ldots, N, \tag{26}$$

where y_i is the decision whether or not to replace the i-th node. All other parameters and variables remain the same as those defined for the formulation IP-4 (given by (19)-(21)). The objective function given in (22) aims to minimize the number of nodes that are to be replaced in the current attempt. Inequality (23) provides the constraint on the available energy for each node (E_0 if the node would be replaced, else E_i). Inequality (24) specifies that the next replacement attempt is no sooner than F days. As an alternative to solving the formulation IP-5 to find the replacement decision in FI policy, we can use a relaxed approach where we will replace the i-th node in a replacement attempt if $E_i < F\ \max\{u_i^1, u_i^2\}$ (use F_{FRD} in place of F for FRD policy). This ensures that none of the nodes will run out of energy in the next F days for any combination of X_1 and X_2. However, this may lead to preventive replacement of a few additional nodes.

We can now use our proposed node replacement policies when any of the ME-1, ME-2 and ME-H routing is used for packet transmission in the network. Since all these combined policies are intractable to study analytically for a network of our size, we take a numerical approach to study their properties. We provide detailed numerical results in the following section.

II.6 Numerical Results

We implemented the proposed routing and node replacement policy combinations on the grid-structured passive seismic network with an inter-node distance of 200 m. Most of the results that we discuss in this section are based on our MATLAB simulations of the given network operation for a time period $T = 50$ years. All MIP/IP formulations are solved using the CPLEX 12 solver. The initial battery energy of a new node is taken as $E_0 = 50000$ J which is close to the amount of energy stored in a MEMS-based compact node currently used in seismic monitoring (SeaBed Geophysical [61]). Considering the cost of this battery and the labor cost associated with the node replacement in deep underwater conditions, the cost of an individual node replacement is approximately estimated as $C = 100$ in appropriate currency units (for example, 100 US dollars). Since the fixed cost of a replacement attempt K is unknown and difficult to estimate, we consider three different cases: $K = 1000,\ 5000$ and 15000. We will assume $K = 5000$ to be a reasonable estimate of a likely cost, and the lower and higher values of K are considered to verify that our approach is still effective for all other values of K.

It is important to see how different routings perform with a particular replacement policy over the range of its fixed parameter (i.e. F in FI, F_{FRD} in FRD and p in FRP). Figure 2 shows such performance comparisons in terms of average maintenance cost of the network for $K = 5000$. The results for the cases $K = 1000$ and $K = 15000$ are found very similar to those for the case $K = 5000$ and hence are not shown.

Figure 2(a) shows how the average maintenance cost changes when we change the replacement interval (F days) in the FI replacement policy. In ME-1 routing, the four nodes at the corners of the lowest level square (see Figure 1(a)) have the fastest energy consumption rate, and they exhaust full battery energy in 70 days. This primarily

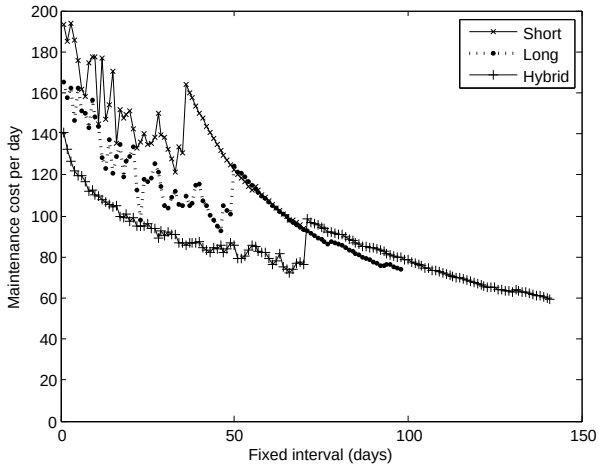

(a) FI

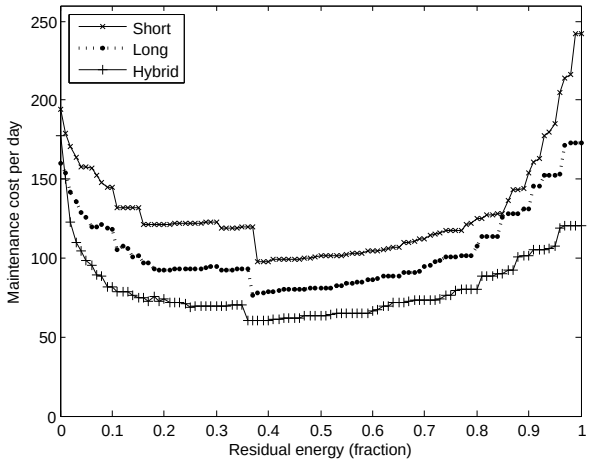

(b) FRP

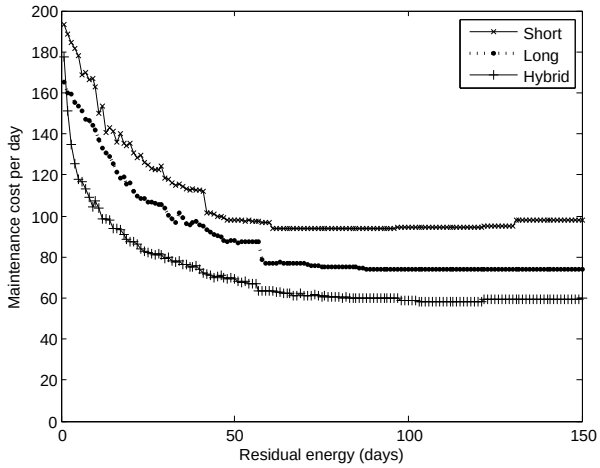

(c) FRD

Figure 2: Average maintenance cost ($T = 50$ years, $E_0 = 50000$ J, $K = 5000$ and $C = 100$)

means that the maximum possible interval in the FI policy for ME-1 routing is 70 days. Similarly, in ME-2 and ME-H routings, only the fastest energy consuming nodes impact the range of F. It can be observed that ME-H routing achieves the lowest average cost among all routings for FI replacement policy. The sharp jumps right after the mid-point of the maximum possible interval can be attributed to more nodes with high residual energy being replaced for those values of F.

Figure 2(b) shows the variations in the average maintenance cost when the threshold energy level (in terms of percentage parameter p) is changed in FRP replacement policy. As expected, with the increase in p value, the average cost first decreases and then increases. The average maintenance cost in FRD policy follows a similar trend (see Figure 2(c)) as we change the fixed parameter F_{FRD}. Based on our argument in the FI policy case, it does not make sense to increase the value of the fixed parameter F_{FRD} in FRD policy beyond the corresponding maximum F values in FI policy for each routing. For example, in the ME-1 routing case, we must make a replacement attempt at least once in every 70 days. Though it is possible to take value of F more than 70 days for this routing with FRD replacement policy, we can see in the plot that the average cost only increases beyond this value of F_{FRD}.

Our idea is ultimately to use the value of the fixed parameter (in the node replacement policy) with which a routing attains the minimum average maintenance cost. We present in Figure 3(a) a comparison of the minimum average maintenance costs obtained from all combinations of our proposed routings and replacement policies for the case $K = 5000$. We have shown that the lowest average maintenance cost is achieved with the ME-H routing in every replacement policy. The ME-2 routing provides a lower average cost than ME-1 routing in most cases, but the ME-H routing is significantly better than both ME-1 and ME-2 routings in all cases. These observations are consistent with our discussions related to network survivability in

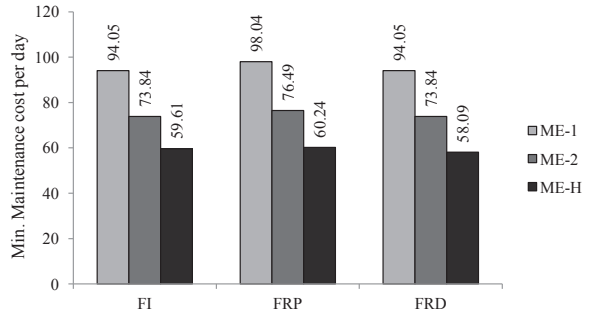

(a) Minimum average maintenance cost

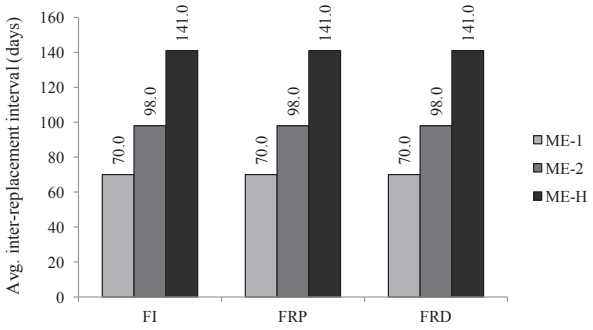

(b) Inter-replacement interval

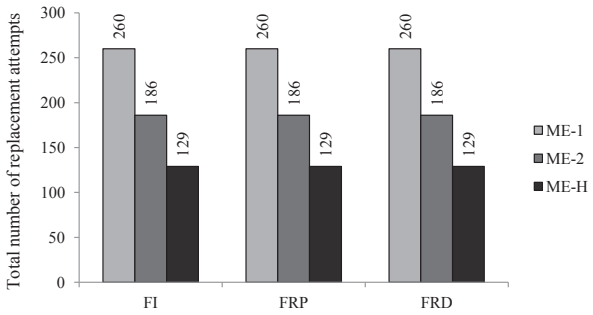

(c) Number of replacement attempts

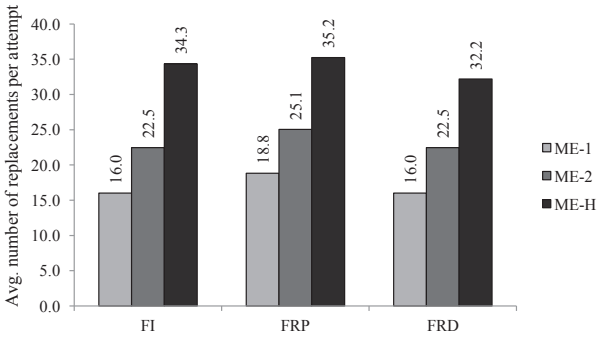

(d) Node replacements per attempt

Figure 3: Performance comparison of policy combinations ($T = 50$ years, $E_0 = 50000$ J, $K = 5000$ and $C = 100$)

Section II.5. Since the fixed cost of a replacement attempt (K) is very high compared to the individual node replacement cost (C), the minimum energy routing that achieves a higher degree of network survivability is also expected to produce a lower average node replacement cost. It can also be observed that FRD replacement policy results in a lower average maintenance cost than FI and FRP policies when a particular routing is kept fixed. Again FI does better than FRP and is close to FRD in minimizing the average replacement cost.

In addition to providing the minimum average maintenance cost, a replacement policy (or schedule) may be required to meet certain service-level criteria. In Figure 3(b)-(d), we present the performance comparison of our proposed policies in terms of important service level parameters for $K = 5000$. The node replacement service will require minimum number of replacement attempts over the period of operation. The inter-replacement interval is also desired to be as long as possible. It can be observed that, in case of most replacement policies, ME-2 routing results in less number of replacement attempts compared to ME-1 routing, but ME-H routing achieves the lowest number of replacement attempts. The ME-H routing also achieves a longer inter-replacement interval with all replacement policies. The observations in Figures 3(a)-3(d) are similar for the cases $K = 1000$ and $K = 15000$ and hence are not shown.

As we know, though the formulation MIP-1 is optimal in minimizing the node replacement costs, this approach can be employed when the number of nodes in the network (N) and the time horizon (T) are small. However, to compare the results of our proposed methods with this optimal solution case, we repeated our experiments for time horizon $T = 25$ days. This was one of the largest instances for which we could solve MIP-1 to optimality within 30 minutes. Also, to ensure a good number of node replacements during this small period of operation, we considered initial

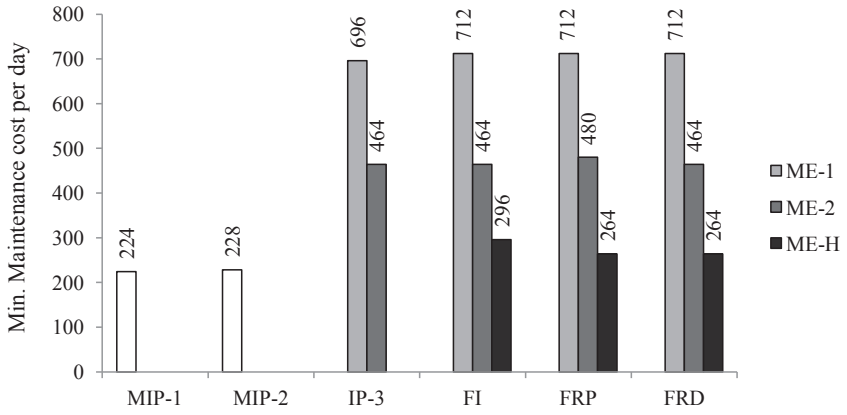

Figure 4: Minimum average maintenance cost ($T = 25$ days, $E_0 = 5000$ J, $K = 5000$ and $C = 100$)

battery energy $E_0 = 5000$ J. For this network setup with $K = 5000$ and $C = 100$, we present in Figure 4 a comparison of minimum average maintenance costs achieved by different approaches that we have considered. As expected, MIP-1 solution provides the lowest average maintenance cost among all approaches considered. As MIP-2 approach considers only fixed routing decisions, the minimum average maintenance cost increases in this case over the MIP-1 solution. When a given fixed routing (e.g. ME-1 and ME-2) is used in the network, IP-3 based solution provides the best results. Also, observe that ME-H routing, when used in combination with our proposed node replacement policies, provides a minimum average maintenance cost that is close to the optimal MIP-1 case. Though this cost gap may look to be considerable in the presented scenario (in Figure 4), this will significantly improve when large values would be considered for the time horizon (T).

We also applied our methods to minimize node replacement costs in an integrated active-passive seismic application. Here passive seismic monitoring is done continuously, and active seismic surveys are conducted once in every few months. Due to closer inter-node spacing requirement for active seismic, we considered a 50

m separation between nodes on our grid network. Note that this network with the reduced inter-node distance is also suitable for passive seismic. The results for this special case are similar to the passive seismic application and hence are not separately presented.

II.7 Conclusion

In this chapter, we developed methods to minimize node replacement costs in underwater wireless sensor networks used in seismic monitoring of undersea oilfields. We introduced the combined routing and node replacement approach to minimize the replacement costs, and developed mathematical formulations that provide the optimal solution. However these MIP/IP formulations become intractable for sizable networks with prolonged seismic monitoring operation. Hence we introduced effective routing and node replacement policies and used them in combinations to achieve the minimum average node replacement cost.

As our numerical results indicate, the ME-H routing with FI or FRD replacement policy provides significantly lower average node replacement cost and meets higher service-level requirements than other joint policies. Though the use of FRD replacement policy with ME-H routing provides the best results, FI policy can still be preferred given its higher degree of simplicity. Also, the difference in the performances of the considered minimum-energy routings ME-1, ME-2 and ME-H is attributed to the varied degree of energy-balancing they achieve. Among the proposed node replacement policies, though the threshold-based FRD policy performs as good as expected, the results also show that using the simple policies like FI in this application is not a bad idea at all. Overall, the main result is that the combined routing and node replacement policy approach is effective and suitable for practical implementation. This approach will also apply to similar permanent monitoring

applications that use remotely located large sensor networks.

We envision many interesting extensions of this work for future research. As an immediate extension, effective methods can be developed to minimize node replacement costs in a generic sensor network. It would also be interesting to see how our methods can be applied to networks that can work with a certain percentage of failed nodes. Additional re-routing routines will be required in this case. The nature of our problem is analogous to a multicomponent maintenance model where the components have both structural and economic dependence. New replacement policies can also be explored in this area.

CHAPTER III

CASE II: MANAGING ENERGY-DELAY TRADE-OFF IN NETWORK CODING FOR WIRELESS TRANSMISSIONS

III.1 Introduction

In recent years, there has been an increasing interest in the applications of network coding in multihop wireless networks (see book by Médard and Sprintson [51] for important application areas). Network coding techniques can significantly reduce the transmission load in wireless networks (Katti *et al.* [35]). For example, consider the two-way relay network shown in Figure 5(a). Here nodes 1 and 2 want to exchange a pair of packets x_1 and x_2 through node 3 which works as a relay node. In the conventional *store-and-forward* approach, node 1 sends its packet x_1 to node 3 which then forwards it to node 2. Similarly packet x_2 is sent from node 2 to node 1 via node 3 in two transmissions. However, in the network coding approach, once the two packets x_1 and x_2 are received at node 3, they are combined by a bit-wise XOR operation, and then the coded packet $x_1 \oplus x_2$ is broadcast to nodes 1 and 2 simultaneously (for example, if $x_1 = 00111100$ and $x_2 = 11001100$, bit-wise XOR operation on x_1 and x_2 results in $x_1 \oplus x_2 = 11110000$). Now, since $x_1 \oplus (x_1 \oplus x_2) = x_2$ and $x_2 \oplus (x_1 \oplus x_2) = x_1$, nodes 1 and 2 can get their required packets by decoding the coded packet. Note that, in this case, a total of 3 transmissions are required compared to 4 transmissions in the conventional approach. In another example, consider a line network with two information flows in opposite directions (see Figure 5(b)). In this case, network coding at successive nodes (known as "reverse carpooling" (Effros *et al.* [20])) allows both flows to share one common path and achieves significant reduction

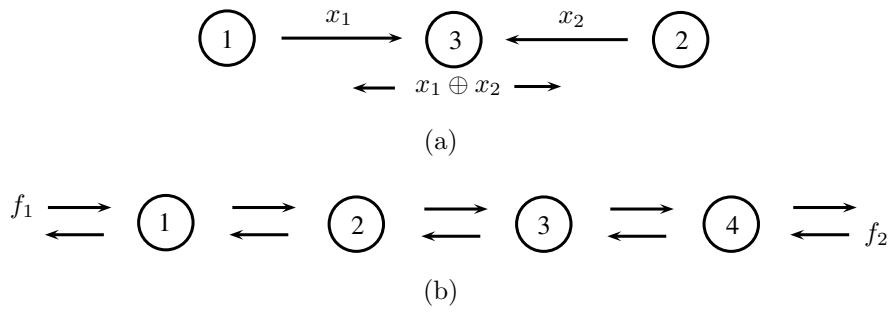

Figure 5: Wireless network coding

in the number of transmissions in the network.

Given the ability of network coding to reduce transmission load greatly, high energy savings are possible by using this technique. This can lead to significant improvements in the energy-efficiency of multihop wireless sensor networks where most of the energy of the nodes is consumed in wireless transmissions. However, in most of these networks, data flows on different links vary significantly. Hence coding opportunities are not always available, and waiting for such opportunities can cause substantial delay in transmission. In fact, the energy savings achieved through network coding may be offset by delays incurred by waiting for coding opportunities. Therefore it is required to decide whether to wait for a coding opportunity or to transmit without coding. To make such decisions, we aim to develop a model to optimally trade-off between low energy consumption and high quality-of-service (i.e. low delay).

In this chapter, we consider the energy-delay trade-off issue in network coding in a two-way relay network (see Figure 5(a)) which is a basic component of larger networks. Our objective is to make network coding decisions at the relay node in such a way that the average energy and delay costs are minimized over the long-run. To achieve this, we formulate our problem as a Markov decision process (MDP) that

takes into account the energy and delay costs as well as the uncertainty in packet arrival processes. A policy for this MDP specifies how many coded and uncoded transmissions are to be made at a transmission opportunity based on the queue backlogs at the relay node. We aim to find the optimal policy in this MDP and develop insights into other simpler policies that can be effective. We will also apply these policies in other network settings such as the one in Figure 5(b).

The remainder of this chapter is organized as follows. We present a brief literature review in Section III.2. In Section III.3, we provide MDP formulations of our problem and show that an optimal stationary policy exists in the average cost MDP. In Section III.4, we derive important structural properties of the optimal policy. In Section III.5, we develop an approach to compute the threshold policy that is optimal in certain cases and is effective (and possibly optimal) in other cases. We report our computational results in Section III.6. Finally, in Section III.7, we present our concluding remarks and some future research directions.

III.2 Literature Review

Network coding has attracted significant interest from the research community since its introduction in the seminal work of Ahlswede *et al.* [2]. However, the energy-delay trade-off issue in network coding has received attention only very recently. He and Yener [23] used a queueing model to analyze this trade-off in a two-way relay network when a first-come-first-serve (FCFS) policy is used for transmission at the relay node. Ciftcioglu *et al.* [17] developed game-based distributed policies to optimize such trade-off in a different relay network setup. Hsu *et al.* [28] developed an MDP based energy-delay trade-off model in a simpler case with a maximum transmission capacity of one packet per time-slot at the relay node.

MDPs serve as efficient methods to optimize cost-performance trade-off in a

stochastic environment (Puterman [56]). There is a rich body of literature on MDPs for various applications. Arapostathis *et al.* [8] provide an extensive survey of works on discrete-time average cost MDPs. In particular, as in our case, it is usually difficult to find an optimal policy (which may also not exist) in average cost MDPs with countably infinite states (hereafter we will say "countable" to mean countably infinite) and unbounded costs. The works by Borkar [12], Cavazos-Cadena [14], Cavasoz-Cadena and Sennott [15], Schäl [60] and Sennott [62, 63, 64] are major contributions to the theory of MDPs with countable state space. In particular, Sennott [63] has provided conditions for existence of an optimal stationary policy in an average cost MDP with countable state space and unbounded costs.

III.3 Model Formulation

We consider network coding in a two-way relay network shown in Figure 6. The relay node R transmits packets between two of its adjacent nodes which have flows in opposite directions. The relay node maintains two queues Q_1 and Q_2 to store packets received from nodes 1 and 2 respectively (i.e. intended for nodes 2 and 1 respectively). Packets arrive at Q_1 and Q_2 according to independent Poisson processes with mean rates λ_1 and λ_2 respectively. The relay node gets opportunity to transmit at fixed time intervals. Let T be the fixed time gap between two consecutive transmission opportunities. The relay node can send any number of packets during a transmission opportunity. However, to save energy, it tries to reduce the number of packet transmissions through network coding. As long as both the queues Q_1 and Q_2 are nonempty, it selects one packet at a time from each queue and combines them as one coded packet which is then broadcast to nodes 1 and 2. When a packet cannot be coded (due to shortage of a packet in the other queue), the relay can transmit it uncoded or hold it for transmission in future. To make this decision, we

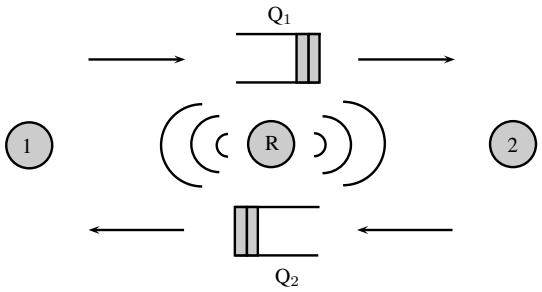

Figure 6: Two-way relay network

consider some costs associated with transmission and delay. Let c_t be the cost of transmitting a coded or uncoded packet, and let $\bar{c}_h$ be the cost of holding a packet per unit time. The cost of holding a packet from one transmission opportunity to the next is $c_h := \bar{c}_h T$. We will consider only the case $c_h < c_t$ since holding will not be a cost-effective option otherwise. However, our analytical results are derived without this assumption.

When each of the queues Q_1 and Q_2 has n packets at a transmission opportunity, it is optimal to transmit n coded packets. When Q_1 has n_1 packets and Q_2 has n_2 ($\neq n_1$) packets, $\min(n_1, n_2)$ coded packets will be sent. However, in this case, since the remaining $|n_1 - n_2|$ packets (that are left in one of the queues) cannot be coded, it is required to decide whether to transmit some of them uncoded. Therefore, our objective is to develop a strategy for the relay to decide how many packets (coded and uncoded) to transmit at every transmission opportunity so that the average transmission and holding cost is minimized over the long-run. To develop such a strategy, we formulate our problem as an MDP which we describe next.

In our MDP setup, the *state* of the system is described by a two-dimensional vector (s_n^1, s_n^2), where s_n^1 and s_n^2 are the number of packets in queues Q_1 and Q_2 respectively just before the n-th ($n = 0, 1, \ldots$) transmission opportunity. The state

space is $\mathcal{S} = \{(i,j) : i = 0,1,\ldots, j = 0,1,\ldots\}$. Based on the state of the system at every stage of the MDP (i.e. at every transmission opportunity), a certain number of coded and uncoded packets are transmitted. Here the total number of packets transmitted is defined as the *action* which is denoted by a_n in the n-th stage. Note that the action space in state (i,j) is $\mathcal{A}_{i,j} = \{\min(i,j), \ldots, \max(i,j)\}$. The complete action space is $\mathcal{A} = \cup_{(i,j)\in\mathcal{S}} \mathcal{A}_{i,j}$. When an action a is taken in state (i,j), the number of coded and uncoded transmissions are $\min(i,j)$ and $a - \min(i,j)$ respectively. Let p_y^z be the probability of y packet arrivals to queue Q_z $(z = 1,2)$ between two transmission opportunities. Note that p_y^1 and p_y^2 $(y = 0,1,\ldots)$ are Poisson probability distributions with means $\lambda_1 T$ and $\lambda_2 T$ respectively. Now, if an action a is taken in state (i,j), the system will be in state (k,l) in the next stage with probability $p_{(i,j)(k,l)}(a) := p^1_{k-(i-a)^+}\, p^2_{l-(j-a)^+}$, where $(x)^+ = \max(x,0)$.

In every stage of the MDP, a transmission cost is incurred depending on the action selected. Further, there is a cost for holding the remaining packets (after transmission) as well as the new arriving packets until the next transmission opportunity. When an action a is taken in state (i,j), the total cost, denoted by $c(i,j,a)$, is computed as

$$c(i,j,a) = c_t a + c_h\left((i-a)^+ + (j-a)^+\right) + \bar{c}_h \mathrm{E}\left[\sum_{z=1}^{2}\sum_{y=1}^{N_z(T)} (T - S_y^z)\right], \qquad (27)$$

where $N_z(T)$ is the random number of new packet arrivals to queue Q_z $(z = 1,2)$ in time T (i.e. in the time between the current and next transmission opportunities), and S_y^z is the time of arrival (measured from the current transmission opportunity) of the y-th packet $(y = 1,\ldots,N_z(T))$ to queue Q_z $(z = 1,2)$. Conditional on $N_z(T) = m$ $(z = 1,2)$, the arrival times $S_1^z,\ldots,S_m^z$ are distributed as the order statistics $U_{(1)},\ldots,U_{(m)}$ of m independent random variables, each uniformly distributed over

$(0, T)$ (Resnick [58]). Using this property of Poisson arrivals, the expression in (27) is simplified as $c(i, j, a) = c_t a + c_h \left((i - a)^+ + (j - a)^+\right) + \frac{c_h T}{2}(\lambda_1 + \lambda_2)$. Note that the cost component $\frac{c_h T}{2}(\lambda_1 + \lambda_2)$ is a constant and will not have any effect on deciding the action in any state. Hence we will ignore it in our model and use the following function for cost per stage.

$$c(i, j, a) = c_t a + c_h \left((i - a)^+ + (j - a)^+\right). \tag{28}$$

Having described the components of the MDP, we need to find a policy that will decide the action at every stage in such a way that the average cost over infinite time horizon will be minimized. A stationary policy for our MDP is a mapping $\theta : \mathcal{S} \to \mathcal{A}$, where $\theta(i, j)$ is the action selected when the state of the system is (i, j). We consider only stationary policies since no better results can be achieved by considering non-stationary policies in time-homogeneous infinite-horizon MDPs (Puterman [56]). The long-run average cost under any policy θ is defined as

$$g(\theta) = \lim_{N \to \infty} \frac{1}{N+1} \mathrm{E}_\theta \left[\sum_{n=0}^{N} c(S_n^1, S_n^2, a_n) \middle| (S_0^1, S_0^2) = (0, 0) \right], \tag{29}$$

where (S_n^1, S_n^2) is random state in the n-th stage. Note that, though we start the system in state $(0, 0)$, the average cost is independent of this choice. Our objective is to find a stationary policy that minimizes the average cost function $g(\theta)$. However, given the countable state space and unbounded costs in our problem, such a policy would exist only under specific conditions.

In the following subsections, we present our analysis to show that an optimal stationary policy exists in our MDP. First, we introduce the discounted cost formulation which is used to derive results for the average cost problem.

III.3.1 Discounted Cost Formulation

In our MDP setup, when a discount factor of β $(0 < \beta < 1)$ is considered, the total expected discounted cost incurred under a policy θ is given by

$$v_{\beta,\theta}(i,j) = \mathrm{E}_\theta \left[\sum_{n=0}^{\infty} \beta^n c(S_n^1, S_n^2, a_n) \middle| (S_0^1, S_0^2) = (i,j) \right], \tag{30}$$

where the initial state of the system is (i,j). The optimal discounted cost in an initial state (i,j) is given by the *discounted cost function* $v_\beta(i,j) := \inf_\theta v_{\beta,\theta}(i,j)$. As per the following proposition, $v_\beta(i,j)$ values are finite.

Proposition 3. *The discounted cost function $v_\beta(i,j)$ is finite for every state $(i,j) \in \mathcal{S}$ and discount factor β $(0 < \beta < 1)$.*

Proof. Consider a policy θ where the decision is to transmit all the queued packets at every transmission opportunity. Note that, under this policy, a total number of $\max(i,j)$ packets will be transmitted in state (i,j). As per (30), the total discounted cost under this policy θ is given by

$$v_{\beta,\theta}(i,j) = c_t \max(i,j) + \mathrm{E}\left[\sum_{n=1}^{\infty} \beta^n c_t \max(A_n^1, A_n^2) \right],$$

where A_n^1 and A_n^2 are the number of packet arrivals to queues Q_1 and Q_2 respectively between the $(n-1)$-st and n-th transmission opportunities. Note that

$$\begin{aligned} v_\beta(i,j) \le v_{\beta,\theta}(i,j) &\le c_t \max(i,j) + \mathrm{E}\left[\sum_{n=1}^{\infty} \beta^n c_t (A_1^n + A_2^n) \right] \\ &= c_t \max(i,j) + \frac{\beta c_t T(\lambda_1 + \lambda_2)}{1-\beta} < \infty. \end{aligned}$$

Since our initial state (i,j) and discount factor β are arbitrary, $v_\beta(i,j) < \infty$ for every

(i,j) and β. $\square$

Proposition 3 implies that the discounted cost function $v_\beta(i,j)$, for $(i,j) \in \mathcal{S}$, satisfies the *discounted cost optimality equation* (DCOE) (Sennott [63]):

$$v_\beta(i,j) \;=\; \min_{a \in \mathcal{A}_{i,j}} \left\{ c(i,j,a) + \beta \sum_{k,l} p_k^1 p_l^2 \; v_\beta\left((i-a)^+ + k, (j-a)^+ + l\right) \right\}. \quad (31)$$

Any stationary policy that realizes the minimum in the right side of (31) is discounted cost optimal. We will use properties of the discounted cost optimal stationary policy to characterize the optimal stationary policy in the average cost case.

III.3.2 Average Cost Formulation

Recall that our objective is to find a stationary policy that minimizes the long-run average cost defined in (29). In this subsection, we show that an average cost optimal stationary policy exists in our MDP, and it can be computed as the limit of discounted cost optimal stationary policies. We will need the following propositions to prove this main result in Theorem 1.

Proposition 4. *The discounted cost function $v_\beta(i,j)$ is nondecreasing in i and j.*

Proof. We will prove this result by using method of induction on the steps of the value iteration algorithm (Puterman [56]). Based on (31), the discounted cost function (for $(i,j) \in \mathcal{S}$) in the n-th step of value iteration is given as

$$v_{\beta,n}(i,j) = \min_{a \in \mathcal{A}_{i,j}} \left\{ c(i,j,a) + \beta \sum_{k,l} p_k^1 p_l^2 \; v_{\beta,n-1}\left((i-a)^+ + k, (j-a)^+ + l\right) \right\}. \quad (32)$$

At the start of value iteration, $v_{\beta,0}(i,j) = 0$ for every state (i,j). Hence, for $n = 0$ case, $v_{\beta,n}(i,j)$ is nondecreasing in i and j.

Now, suppose $n-1$ case is true, i.e. $v_{\beta,n-1}(i,j)$ is nondecreasing in i and j. Using (32), select an action $a \in \mathcal{A}_{i+1,j}$ such that

$$v_{\beta,n}(i+1,j) = c(i+1,j,a) + \beta \sum_{k,l} p_k^1 p_l^2 \; v_{\beta,n-1}\left((i+1-a)^+ + k, (j-a)^+ + l\right). \quad (33)$$

For the same action a, we must have from (32):

$$v_{\beta,n}(i,j) \leq c(i,j,a) + \beta \sum_{k,l} p_k^1 p_l^2 \; v_{\beta,n-1}\left((i-a)^+ + k, (j-a)^+ + l\right). \quad (34)$$

Note that $a \notin \mathcal{A}_{i,j}$ when $a = i+1 > j$, but (34) will still hold. Since $v_{\beta,n-1}(i,j)$ and $c(i,j,a)$ (see (28)) are nondecreasing in i, we use (33) and (34) to show that

$$\begin{aligned} v_{\beta,n}(i+1,j) - v_{\beta,n}(i,j) \;\geq\; & c(i+1,j,a) - c(i,j,a) \\ & + \beta \sum_{k,l} p_k^1 p_l^2 \; \Big\{ v_{\beta,n-1}\left((i+1-a)^+ + k, (j-a)^+ + l\right) \\ & - v_{\beta,n-1}\left((i-a)^+ + k, (j-a)^+ + l\right) \Big\} \geq 0. \end{aligned}$$

Hence $v_{\beta,n}(i,j)$ is nondecreasing in i for any fixed j. Similarly we can show that $v_{\beta,n}(i,j)$ is nondecreasing in j for any fixed i. Thus $v_{\beta,n}(i,j)$ is nondecreasing in both i and j. Therefore the discounted cost function $v_\beta(i,j)$ is nondecreasing in i and j, as $v_{\beta,n}(i,j) \to v_\beta(i,j)$. □

Proposition 5. *The MDP has a stationary policy inducing an irreducible, ergodic Markov chain with a finite average cost.*

Proof. Consider again the policy θ where the decision is to transmit all the queued packets at every transmission opportunity. Under this policy, the state of the system $\{(S_n^1, S_n^2), n \geq 0\}$ can be described by an irreducible and ergodic Markov chain with

transition probabilities $p_{(i,j)(k,l)} := p_k^1 p_l^2$ for $(i,j),(k,l) \in \mathcal{S}$. Note that the stationary distribution of this Markov chain is $\pi_{i,j} := p_i^1 p_j^2$ for $(i,j) \in \mathcal{S}$. Therefore the long-run average cost under policy θ is given by

$$g(\theta) = \sum_{(i,j)\in\mathcal{S}} \pi_{i,j}\ c_t \max(i,j) \leq c_t \sum_{i=0}^{\infty}\sum_{j=0}^{\infty} p_i^1 p_j^2 (i+j) = c_t(\lambda_1+\lambda_2)T < \infty.$$

This shows that the average cost in the considered policy is finite. □

Theorem 1. *(a) There exist a constant $g = \lim_{\beta\uparrow 1}\ (1-\beta)v_\beta(i,j)$ for every $(i,j) \in \mathcal{S}$, and a function $h(i,j)$ satisfying the average cost optimality inequality (ACOI):*

$$g + h(i,j) \geq \min_{a\in\mathcal{A}_{i,j}} \left\{ c(i,j,a) + \sum_{k,l} p_k^1 p_l^2\ h\left((i-a)^+ + k, (j-a)^+ + l\right) \right\}. \qquad (35)$$

The constant g is the optimal average cost, and any stationary policy that realizes the minimum in the right side of (35) is average cost optimal.
(b) There exists an average cost optimal stationary policy θ^* that is a limit point of a sequence of discounted cost optimal stationary policies $\{\theta_{\beta_k}\}_{k\geq 1}$, where $\beta_k \to 1$.

Proof. To prove (a) and (b), we will first show that the following conditions (provided by Sennott [63]) are satisfied.

1. The discounted cost function $v_\beta(i,j)$ is finite for every state (i,j) and discount factor β.

2. There exists a nonnegative number N such that $-N \leq h_\beta(i,j)$ for all (i,j) and β, where $h_\beta(i,j) = v_\beta(i,j) - v_\beta(0,0)$.

3. There exist nonnegative numbers M_{ij} such that $h_\beta(i,j) \leq M_{ij}$ for every (i,j) and β. Also, for every state (i,j), there exists an action $a(i,j)$ such that $\sum_{(k,l)\in\mathcal{S}}\ p_{(i,j)(k,l)}(a(i,j))\ M_{kl} < \infty$.

Condition 1 is satisfied through Proposition 3. Condition 2 is implied by Proposition 4 and is therefore satisfied. Based on Proposition 5 in Sennott [63], Proposition 5 satisfies Condition 3. Now that Conditions 1-3 are satisfied, the result in (a) follows from Theorem 7.2.3 (and its proof) in Sennott [65].

Now, let $\{\beta_n\}_{n\geq 1}$ be any sequence of discount factors converging to 1, and let $\{\theta_{\beta_n}\}_{n\geq 1}$ be the corresponding sequence of discounted cost optimal stationary policies. By Lemma 1 in Sennott [63], there exists a subsequence of discount factors $\{\beta_{n_k}\}_{k\geq 1}$ (also converging to 1) and a stationary policy θ^* that is a limit point of the subsequence $\{\theta_{\beta_{n_k}}\}_{k\geq 1}$. Further, as Conditions 1-3 are satisfied, the stationary policy θ^* is average cost optimal by Theorem 1 in Sennott [63]. □

III.4 Structural Properties of Optimal Policy

In this section, we derive structural properties of the optimal policy in both discounted cost and average cost problems. In Theorem 1, we showed that an average cost optimal stationary policy in our MDP can be found as a limit point of discounted cost optimal stationary policies. Therefore structural properties of the discounted cost optimal stationary policies will remain the same in this average cost optimal stationary policy.

Before formalizing our main results, we would like to introduce certain concepts of convexity of a function defined over discrete points. First, we define a univariate "discrete convex function" for our purpose.

Definition 1. *The function $f : \mathbb{Z}_+ \to \mathbb{R}$ is defined to be convex if and only if $f(i+1) - f(i)$ is nondecreasing in i.*

If $f : \mathbb{Z}_+ \to \mathbb{R}$ is convex (by Definition 1), a point i in the domain of f is a global minimum if it is a local minimum in the sense that $f(i) \leq \min\{f(i-1), f(i+1)\}$. This function will also satisfy other natural properties of a convex function (Murota

[52]). Now we extend the idea in Definition 1 to a bivariate discrete function in which we are primarily interested in analyzing convexity in the direction of one variable.

Definition 2. *The function $f : \mathbb{Z}_+^2 \to \mathbb{R}$ is defined to be convex in i if and only if $f(i+1,j) - f(i,j)$ is nondecreasing in i for every j. Similarly, f is defined to be convex in j if and only if $f(i,j+1) - f(i,j)$ is nondecreasing in j for every i.*

Note that, if $f(i,j)$ is convex in i (by Definition 2), then for a fixed j (say j_1), the function $f_1(i) := f(i,j_1)$ is convex. Similarly, if $f(i,j)$ is convex in j, then for a fixed i (say i_1), the function $f_2(j) := f(i_1,j)$ is convex. Additionally, if $f(i,j)$ and $g(i,j)$ are convex in i (resp. in j), the function $c_1 f(i,j) + c_2 g(i,j)$ is convex in i (resp. in j) for $c_1 \geq 0, c_2 \geq 0$. We will use these properties in the proofs of various results presented in this section.

Definition 2 helps check convexity of a bivariate discrete function in only one variable (while the other is fixed), which is useful for deriving our results. However note that, even if a function is convex in each variable separately, it is not sufficient to identify the function as convex unless it is additively separable.

Now we present in the following Lemma 1 and Proposition 6 that are required to prove the main result of this section in Theorem 2.

Lemma 1. *Suppose $f(i,j) : \mathbb{Z}_+^2 \to \mathbb{R}$ is convex in i and j. For $c > 0$, the function $g(i,j) = \min_{a \in \{\min(i,j),\ldots,\max(i,j)\}} \{ca + f((i-a)^+, (j-a)^+)\}$ is convex in i and j if*

$$\min\{f(1,0) - f(0,0), c\} + \min\{f(0,1) - f(0,0), c\} \geq c. \tag{36}$$

Proof. When $i \geq j$, we have

$$g(i,j) \;=\; \min_{a \in \{j,\ldots,i\}} \{ca + f(i-a,0)\} = ci + \min_{k \in \{0,\ldots,i-j\}} f_1(k),$$

where $f_1(k) = -ck + f(k,0)$. Since the functions $-ck$ and $f(k,0)$ are convex (by Definition 1), $f_1(k)$ is convex. Let $k_1^* = \arg\min\{f_1(k) : k \geq 0\}$ be a global minimum of the function f_1. Using convexity of f_1, we have

$$g(i,j) = \begin{cases} ci + f_1(i-j) & \text{if } 0 \leq i-j < k_1^*, \\ ci + f_1(k_1^*) & \text{if } i-j \geq k_1^*. \end{cases} \tag{37}$$

Similarly, when $i \leq j$, we can show that there exists a $k_2^* \geq 0$ such that

$$g(i,j) = \begin{cases} cj + f_2(j-i) & \text{if } -k_2^* < i-j \leq 0, \\ cj + f_2(k_2^*) & \text{if } i-j \leq -k_2^*, \end{cases} \tag{38}$$

where $f_2(k) = -ck + f(0,k)$. Also note that $f_1(0) = f_2(0) = f(0,0)$.

Now, by Definition 2, the function $g(i,j)$ will be convex in i and j, if

$$g(i+1,j) - g(i,j) \geq g(i,j) - g(i-1,j), \qquad i \geq 1, j \geq 0, \tag{39}$$

$$g(i,j+1) - g(i,j) \geq g(i,j) - g(i,j-1), \qquad i \geq 0, j \geq 1. \tag{40}$$

We will show that (39) and (40) hold in all the following cases: (a) $i > j$, (b) $i < j$, and (c) $i = j$.

First, in case (a) $i > j$, we consider two sub-cases: (a1) $0 < i-j < k_1^*$, and (a2) $i - j \geq k_1^*$. In sub-case (a1) $0 < i-j < k_1^*$, using (37) and convexity of f_1, we show in the following that (39) and (40) are satisfied.

$$\begin{aligned} g(i+1,j) - g(i,j) &= c(i+1) + f_1(i-j+1) - ci - f_1(i-j) \\ &\geq [ci + f_1(i-j)] - [c(i-1) + f_1(i-j-1)] \\ &= g(i,j) - g(i-1,j). \end{aligned}$$

$$\begin{aligned} g(i,j+1) - g(i,j) &= ci + f_1(i-j-1) - ci - f_1(i-j) \\ &\geq [ci + f_1(i-j)] - [ci + f_1(i-j+1)] \\ &= g(i,j) - g(i,j-1). \end{aligned}$$

Also, in sub-case (a2) $i - j \geq k_1^*$, we show below that (39) and (40) are satisfied.

$$\begin{aligned} g(i+1,j) - g(i,j) &= c(i+1) + f_1(k_1^*) - ci - f_1(k_1^*) \\ &= [ci + f_1(k^*)] - [c(i-1) + f_1(k_1^*)] \\ &\geq g(i,j) - g(i-1,j). \\ g(i,j+1) - g(i,j) &\geq [ci + f_1(k^*)] - [ci + f_1(k_1^*)] \\ &= g(i,j) - g(i,j-1). \end{aligned}$$

Thus both (39) and (40) are satisfied in case (a) $i > j$. Similarly, by using (38) and convexity of f_2, we can show that these conditions are also satisfied in case (b) $i < j$. In case (c) $i = j$, note that (37) will hold if

$$\begin{aligned} & g(i+1,i) - g(i,i) \geq g(i,i) - g(i-1,i), \\ \text{i.e.} \quad & \min\{ci + f(1,0), c(i+1) + f(0,0)\} - ci - f(0,0) \\ & \geq ci + f(0,0) - \min\{c(i-1) + f(0,1), ci + f(0,0)\}, \\ \text{i.e.} \quad & \min\{f(1,0) - f(0,0), c\} + \min\{f(0,1) - f(0,0), c\} \geq c, \end{aligned}$$

which is the condition specified in (36). Similarly it can be shown that, when this condition holds, we also have $g(i,i+1) - g(i,i) \geq g(i,i) - g(i,i-1)$.

Thus, given that (36) holds, $g(i,j)$ satisfies (39) and (40) at all points. Therefore $g(i,j)$ is convex in i and j. □

Proposition 6. *If $c_h \geq c_t/2$, the cost function $v_\beta(i,j)$ is convex in i and j.*

Proof. We will prove this result by using method of induction on the steps of the value iteration algorithm. The discounted cost function in the n-th step of value iteration is given by

$$\begin{aligned} v_{\beta,n}(i,j) &= \min_{a\in\mathcal{A}_{i,j}} \Big\{ c_t a + c_h \left[(i-a)^+ + (j-a)^+\right] \\ &\quad +\beta \sum_{k,l} p_k^1 p_l^2 \; v_{\beta,n-1}\left((i-a)^+ + k, (j-a)^+ + l\right) \Big\}, \; (i,j) \in \mathcal{S}. \quad (41) \end{aligned}$$

At the start of value iteration, $v_{\beta,0}(i,j) = 0$ for every state (i,j). Hence, for $n = 0$ case, $v_{\beta,n}(i,j)$ is convex in i and j. Now, suppose $n-1$ case is true, i.e. $v_{\beta,n-1}(i,j)$ is convex in i and j. Therefore the function $f_{n-1}(i,j) := \sum_{k,l} \; p_k^1 p_l^2 \; v_{\beta,n-1}(i+k, j+l)$ is convex in i and j. Now we can write (41) as

$$v_{\beta,n}(i,j) = \min_{a\in\mathcal{A}_{i,j}} \Big\{ c_t a + g_{n-1}\left((i-a)^+, (j-a)^+\right) \Big\}, \quad (42)$$

where $g_{n-1}(i,j) = c_h(i+j) + \beta f_{n-1}(i,j)$. Since $c_h(i+j)$ and $f_{n-1}(i,j)$ are convex in i and j, $g_{n-1}(i,j)$ is convex in i and j. Therefore by Lemma 1, in (42), $v_{\beta,n}(i,j)$ is convex in i and j if

$$\min\{g_{n-1}(1,0) - g_{n-1}(0,0), c_t\} + \min\{g_{n-1}(0,1) - g_{n-1}(0,0), c_t\} \geq c_t. \quad (43)$$

Since $v_{\beta,n}(i,j)$ is nondecreasing in i and j in every stage of value iteration (see proof of Proposition 4), we have

$$g_{n-1}(1,0) - g_{n-1}(0,0) \;=\; c_h + \beta \sum_{k,l} p_k^1 p_l^2 \; [v_{\beta,n-1}(k+1,l) - v_{\beta,n-1}(k,l)] \geq c_h, \quad (44)$$

$$g_{n-1}(0,1) - g_{n-1}(0,0) \;=\; c_h + \beta \sum_{k,l} p_k^1 p_l^2 \;\left[v_{\beta,n-1}(k,l+1) - v_{\beta,n-1}(k,l)\right] \geq c_h. \tag{45}$$

Using (44) and (45), the sufficient condition for (43) to hold is $2c_h \geq c_t$. However, this is the necessary condition in case $n = 1$ where (44) and (45) are satisfied at equality. Thus $v_{\beta,n}(i,j)$ is convex in i and j if $c_h \geq c_t/2$. Therefore, under the same condition, the discounted cost function $v_\beta(i,j)$ is convex in i and j, as $v_{\beta,n}(i,j) \to v_\beta(i,j)$. $\square$

Theorem 2. *If $c_h \geq c_t/2$, then (a) there exist constants $L_1, L_2 \geq 0$ (corresponding to every discount factor β) such that the optimal action in state $(i,j) \in \mathcal{S}$ in the discounted cost problem is given by*

$$a^*(i,j) = \min(i,j) + (i - \min(i,j) - L_1)^+ + (j - \min(i,j) - L_2)^+ . \tag{46}$$

(b) There is an average cost optimal policy which has the same structure as the discounted cost optimal policy specified in (46).

Proof. Since $a \in \mathcal{A}_{i,j} = \{\min(i,j), \ldots, \max(i,j)\}$, we can write $a = \max(i,j) - (i - a)^+ - (j - a)^+$. Using this, (31) can be written for every $(i,j) \in \mathcal{S}$ as

$$\begin{aligned} v_\beta(i,j) \;=\; & c_t \max(i,j) + \min_{a \in \mathcal{A}_{i,j}} \Big\{ -(c_t - c_h)\left[(i-a)^+ + (j-a)^+\right] \\ & + \beta \sum_{k,l} p_k^1 p_l^2 \; v_\beta\left((i-a)^+ + k, (j-a)^+ + l\right) \Big\}. \end{aligned} \tag{47}$$

Since $c_h \geq c_t/2$, the discounted cost function $v_\beta(i,j)$ is convex in i and j by Proposition 6. Therefore the function $f(i,j) := \sum_{k,l} \; p_k^1 p_l^2 \; v_\beta(i+k, j+l)$ is convex in i and j. Also, it can be shown that $-(c_t - c_h)(i+j)$ is convex in i and j. Now we can

write (47) as

$$v_\beta(i,j) = c_t \max(i,j) + \min_{a \in \mathcal{A}_{i,j}} \Big\{ g\left((i-a)^+, (j-a)^+\right) \Big\}, \tag{48}$$

where $g(i,j) = -(c_t - c_h)(i+j) + \beta f(i,j)$. Note that $g(i,j)$ is convex in i and j.

Now, we will prove result (a) by considering the following cases: (i) $i \geq j$, and (ii) $i \leq j$. In case (i) $i \geq j$, (48) can be written as

$$v_\beta(i,j) = c_t \max(i,j) + \min_{a \in \{j,\ldots,i\}} g(i-a,0) = c_t \max(i,j) + \min_{b \in \{0,\ldots,i-j\}} g_1(b), \tag{49}$$

where $b = i - a$, and $g_1(b) = g(b,0)$. Note that $g_1(b)$ is convex. Let $L_1 = \arg\min\{g_1(b) : b \geq 0\}$ be a global minimum of $g_1(b)$. Hence the value of b that minimizes $g_1(b)$ in (49) is given by

$$b^*(i,j) = \begin{cases} i-j & \text{if } 0 \leq i-j < L_1, \\ L_1 & \text{if } i-j \geq L_1. \end{cases}$$

Therefore, in case (i) $i \geq j$, the optimal action in state (i,j) can be found as

$$a^*(i,j) = i - b^*(i,j) = \begin{cases} j & \text{if } 0 \leq i-j < L_1, \\ i-L_1 & \text{if } i-j \geq L_1. \end{cases} \tag{50}$$

Similarly, in case (ii) $i \leq j$, it can be shown that there exists a constant $L_2 \geq 0$ such that the optimal action in state (i,j) is given by

$$a^*(i,j) = \begin{cases} i & \text{if } 0 \leq j-i < L_2, \\ j-L_2 & \text{if } j-i \geq L_2. \end{cases} \tag{51}$$

Note that (50) and (51) can be combined into one expression as presented in (46). This completes the proof of the result (a). Result (b) follows from Theorem 1(b). □

Theorem 2 shows that, if $c_h \geq c_t/2$, the optimal transmission policy for the relay node is a special kind of threshold policy whose structure is specified in (46). Observe that, under such a policy, $\min(i, j)$ coded packets are sent in state (i, j) as in any other policy. However, once the coded packets are sent, packets from the nonempty queue are sent uncoded until the number of remaining packets in the queue reaches an optimal threshold level (say L_1^* for Q_1 and L_2^* for Q_2 in the average cost case).

Notice that the condition $c_h \geq c_t/2$ is only sufficient, but not necessary, for the optimal policy to be threshold-based. We have not shown whether such threshold policy is optimal when $c_h < c_t/2$. However, in this case, we expect the optimal action $a^*(i, j)$ to be nondecreasing in i and j in a way similar to this threshold policy. Hence, when $c_h < c_t/2$, we believe that the threshold policy will be very effective, if not optimal. We provide evidence for this in our numerical results (Section III.6).

Note that an individual packet incurs a transmission cost of $c_t/2$ if it is coded, and c_t if it is sent uncoded. Hence a packet cannot reduce its own cost by waiting for a coding opportunity if $c_h + c_t/2 \geq c_t$ or $c_h \geq c_t/2$. Therefore, under the condition $c_h \geq c_t/2$, the *individually optimal* average cost policy is to always transmit (coded if possible, else uncoded) at a transmission opportunity. However, it is clear from Theorem 2 that this policy may not be optimal at the system level.

III.5 Computation of Threshold Policy

Given the countable state space in our MDP, computing the optimal stationary policy (in both discounted cost and average cost problems) by standard value iteration or policy iteration procedures is intractable. However, now we know that the average cost optimal policy is threshold-based if $c_h \geq c_t/2$. Also, such a threshold

policy will be efficient (and possibly optimal) in the case $c_h < c_t/2$. Therefore we are primarily interested in computing the threshold policy in all cases. Here, by threshold policy, we mean the best threshold policy, i.e. optimal values of the thresholds are used. In this section, we develop an approach to compute the optimal threshold values L_1^* and L_2^* which completely characterize the threshold policy.

Consider in our MDP an arbitrary threshold policy with threshold values L_1 and L_2 (where $L_1 \geq 0, L_2 \geq 0$). In this (L_1, L_2) threshold policy, the action in state $(i, j) \in \mathcal{S}$ is specified in (46). Under this policy, let Z_n^1 and Z_n^2 denote the number of packets in queues Q_1 and Q_2 respectively just after all transmissions are completed in the n-th transmission opportunity. Note that the stochastic process $\{(Z_n^1, Z_n^2), n \geq 0\}$ is an irreducible discrete-time Markov chain with state space $\mathcal{S}' = \{(0, L_2), (0, L_2 - 1), \ldots, (0, 1), (0, 0), (1, 0), \ldots, (L_1 - 1, 0), (L_1, 0)\}$. The transition probabilities in this Markov chain are given by

$$
\begin{aligned}
\bar{p}_{(i,0)(k,0)} &= q_{(k-i)}, && 0 \leq i \leq L_1,\ 0 \leq k < L_1, \\
\bar{p}_{(i,0)(L_1,0)} &= \sum_{m \geq L_1 - i} q_m, && 0 \leq i \leq L_1, \\
\bar{p}_{(i,0)(0,l)} &= q_{-(i+l)}, && 0 \leq i \leq L_1,\ 0 \leq l < L_2, \\
\bar{p}_{(i,0)(0,L_2)} &= \sum_{m \leq -(i+L_2)} q_m, && 0 \leq i \leq L_1, \\
\bar{p}_{(0,j)(0,l)} &= q_{-(l-j)}, && 0 \leq j \leq L_2,\ 0 \leq l < L_2, \\
\bar{p}_{(0,j)(0,L_2)} &= \sum_{m \leq -(L_2 - j)} q_m, && 0 \leq j \leq L_2, \\
\bar{p}_{(0,j)(k,0)} &= q_{(j+k)}, && 0 \leq k < L_1,\ 0 \leq j \leq L_2, \\
\bar{p}_{(0,j)(L_1,0)} &= \sum_{m \geq j + L_1} q_m, && 0 \leq j \leq L_2,
\end{aligned}
$$

where q_m is the probability of Q_1 receiving m (where m is an integer in $(-\infty, \infty)$) more packets than Q_2 between two transmission opportunities. Note that q_m is

the probability distribution of the difference of two independent Poisson random variables, and it is specified by the Skellam distribution (Skellam [70]):

$$q_m = e^{-(\lambda_1+\lambda_2)T}\left(\frac{\lambda_1}{\lambda_2}\right)^{m/2} I_{|m|}(2T\sqrt{\lambda_1\lambda_2}),$$

where $I_{(\cdot)}(\cdot)$ is the modified Bessel function of the first kind.

Note that the long-run average cost incurred in the considered Markov chain is precisely the average cost under (L_1, L_2) threshold policy in our MDP. The expected cost incurred in state $(i, j) \in \mathcal{S}'$ of the Markov chain is given by

$$\begin{aligned} c_{ij}(L_1, L_2) &= \sum_{k,l} p_k^1 p_l^2 \Big\{ c_h(i+j) + c_t\Big[\min(i+k, j+l) \\ &\quad + (i+k-\min(i+k, j+l) - L_1)^+ \\ &\quad + (j+l-\min(i+k, j+l) - L_2)^+ \Big]\Big\}. \end{aligned}$$

Now the long-run average cost under (L_1, L_2) threshold policy can be calculated as

$$\bar{g}(L_1, L_2) = \sum_{(i,j)\in\mathcal{S}'} \bar{\pi}_{ij} c_{ij}(L_1, L_2), \tag{52}$$

where $\{\bar{\pi}_{ij} : (i, j) \in \mathcal{S}'\}$ is the set of stationary probabilities of the Markov chain satisfying the equations $\sum_{(k,l)\in\mathcal{S}'} \bar{\pi}_{kl}\bar{p}_{(k,l)(i,j)} = \bar{\pi}_{ij}$, for all $(i, j) \in \mathcal{S}'$, and $\sum_{(i,j)\in\mathcal{S}} \bar{\pi}_{ij} = 1$.

Now the optimal values of the thresholds, L_1^* and L_2^*, can be found by minimizing the discrete function $\bar{g}(L_1, L_2)$ in (52). As a simple approximation method, the global minimum of $\bar{g}(L_1, L_2)$ can be found by evaluating this function over a finite set $\{0, 1, \ldots, N_1\} \times \{0, 1, \ldots, N_2\}$, where N_1 and N_2 are suitably large integers. However, in our numerical experiments, a local minimum of $\bar{g}(L_1, L_2)$ was found to be the global minimum in all cases. Assuming that $\bar{g}(L_1, L_2)$ has this property, any discrete

gradient search method can be applied to find the minimum (L_1^*, L_2^*) more efficiently.

III.6 Numerical Results

In this section, we present our numerical results to demonstrate the effectiveness of the threshold policy in network coding decisions. Most of the results presented in this section are based on our MATLAB simulations of node/network operation covering a large number of transmission opportunities. The objective in these experiments is to compare the threshold policy against other simple policies, and test these policies in situations where assumptions do not hold. We mainly study the performance of the following policies.

1. *Transmit-all Policy*: Under this policy, the relay node transmits all the queued packets at every transmission opportunity. In this case, like every other policy, when the relay has i and j packets in queues Q_1 and Q_2 respectively, $\min(i, j)$ coded packets are sent. Then all the remaining packets (that are left in one of the queues) are sent uncoded.

2. *Rate-based Policy*: This policy is based on λ_1 and λ_2 which are the mean rates of packet arrivals (Poisson distributed) to Q_1 and Q_2 respectively. Under this policy, upon transmission of coded packets, all the remaining packets in Q_1 (if it is nonempty) are sent uncoded if $\lambda_1 > \lambda_2$, and are held if $\lambda_1 < \lambda_2$. Similarly, if Q_2 is nonempty following transmission of coded packets, all its remaining packets are sent unocoded if $\lambda_1 < \lambda_2$, and are held if $\lambda_1 > \lambda_2$. We will not use this policy when $\lambda_1 = \lambda_2$.

3. *Threshold Policy*: Here we mean the best (L_1, L_2) threshold policy, i.e. optimal values of the thresholds (L_1^* and L_2^*) are used. Recall that this is the optimal transmission policy for the relay node if $c_h \geq c_t/2$.

Note that both "transmit-all" and "rate-based" policies are special instances of the (L_1, L_2) threshold policy (see (46)). In the "transmit-all" policy, we have $(L_1, L_2) = (0, 0)$. In the "rate-based" policy, $(L_1, L_2) = (0, \infty)$ if $\lambda_1 > \lambda_2$, and $(L_1, L_2) = (\infty, 0)$ if $\lambda_1 < \lambda_2$. Since these policies are specific threshold policies, they will not perform any better than the best threshold policy (which we call just the "threshold policy"). However, since these policies are easy to implement (as the values of the thresholds L_1 and L_2 are already known), we would like to find out how efficient they are.

We computed the threshold policy for a relay node using our approach described in Section III.5. Table 2 presents the threshold values (L_1^* and L_2^*) in the computed threshold policy for different values of mean arrival rates λ_1 and λ_2, and cost parameters c_t and c_h. We use $c_t = 1$ and $T = 1$ in all our results. Notice that $L_1^* > L_2^*$ whenever $\lambda_1 < \lambda_2$. This is because, when $\lambda_1 < \lambda_2$, packets in Q_1 have higher chances of being coded than those in Q_2, and therefore the holding option is more appealing to Q_1 than Q_2. Likewise we have $L_1^* < L_2^*$ if $\lambda_1 > \lambda_2$, though instances of this case are not shown. Observe that, for fixed values of c_t and c_h, as λ_2 increases over λ_1, value of L_1^* increases, and value of L_2^* decreases. Similarly, if λ_1 increases over λ_2, value of L_1^* will decrease, and value of L_2^* will increase. This trend suggests that the threshold policy will be close to the "rate-based" policy when $\lambda_1 << \lambda_2$ or $\lambda_1 >> \lambda_2$. Also observe that, when values of λ_1 and λ_2 are fixed, both L_1^* and L_2^* values decrease as the holding cost quantity c_h increases. This is expected since fewer packets will be held when the holding cost is more. When c_h is considerably high, we have $L_1^* = L_2^* = 0$. In this case, the threshold policy is precisely the "transmit-all" policy.

Based on our simulation results, Figure 7 presents comparison of the long-run average costs of the policies in different instances of λ_1 and λ_2. Since the holding cost quantity c_h is usually not known explicitly, we compare the average costs of

Table 2: Computed threshold policy

λ_1	λ_2	c_h	c_t	L_1^*	L_2^*	Avg. cost
5	5	0.05	1	8	8	5.4931
5	5	0.1	1	5	5	5.6875
5	5	0.2	1	3	3	5.9439
5	5	0.4	1	1	1	6.2138
5	5	0.6	1	0	0	6.2455
5	5.5	0.05	1	14	4	5.7952
5	5.5	0.1	1	8	3	5.9814
5	5.5	0.2	1	4	2	6.2331
5	5.5	0.4	1	1	0	6.4996
5	5.5	0.6	1	0	0	6.5422
5	6	0.05	1	21	2	6.1750
5	6	0.1	1	11	1	6.3270
5	6	0.2	1	6	1	6.5510
5	6	0.4	1	2	0	6.7908
5	6	0.6	1	0	0	6.8669
5	7.5	0.05	1	48	0	7.5480
5	7.5	0.1	1	23	0	7.5960
5	7.5	0.2	1	11	0	7.6908
5	7.5	0.4	1	4	0	7.8520
5	7.5	0.6	1	2	0	7.9542

the policies over different possible values of c_h/c_t. Notice that, as expected, the threshold policy always achieves the minimum average cost among the considered policies. However, the "transmit-all" and "rate-based" policies perform as good as the threshold policy in certain situations. When both arrival rates λ_1 and λ_2 are very small, the "transmit-all" policy is very effective at almost all values of c_h (see Figure 7(a)). When the difference between λ_1 and λ_2 is large, the "rate-based" policy performs very close to the threshold policy at most values of c_h (see Figure 7(d)). In all other cases of λ_1 and λ_2, the "rate-based" policy is effective at very low values of

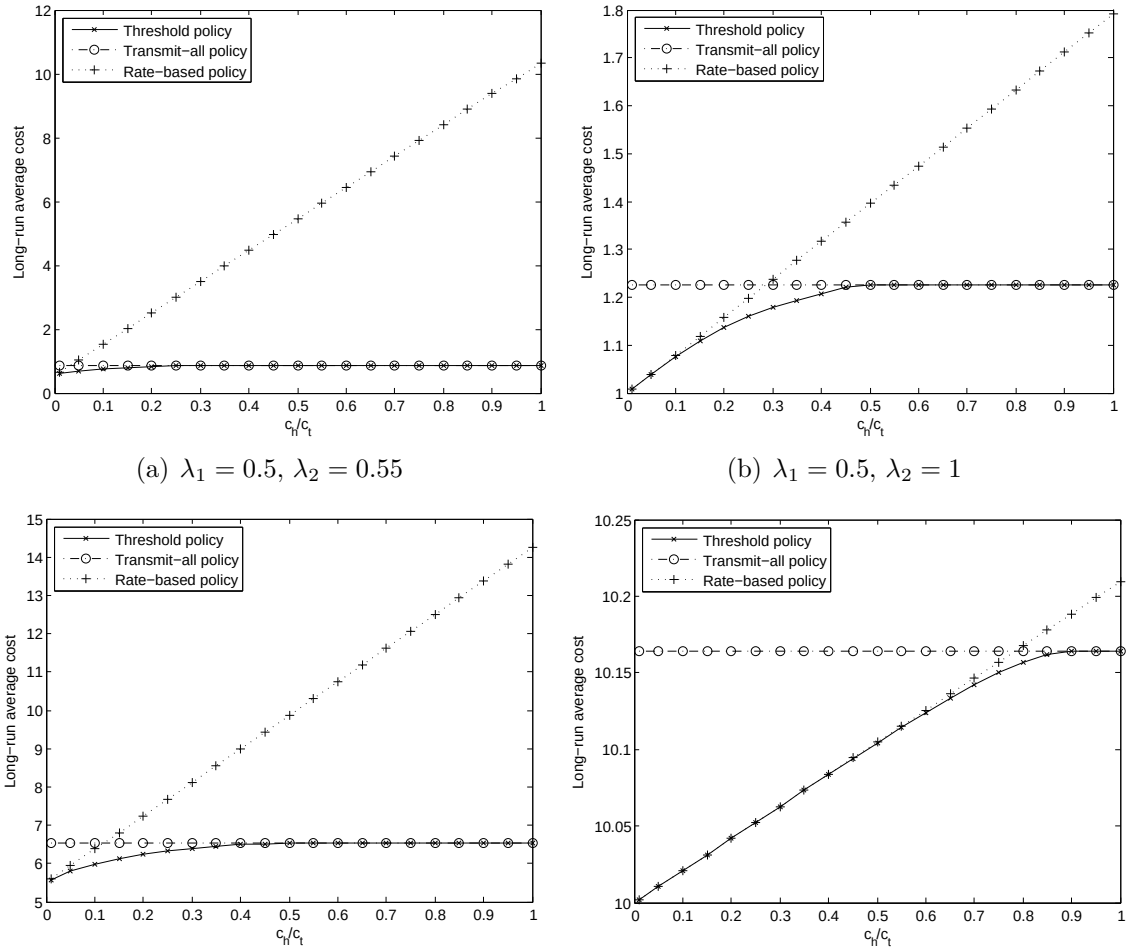

(a) $\lambda_1 = 0.5$, $\lambda_2 = 0.55$

(b) $\lambda_1 = 0.5$, $\lambda_2 = 1$

(c) $\lambda_1 = 5$, $\lambda_2 = 5.5$

(d) $\lambda_1 = 5$, $\lambda_2 = 10$

Figure 7: Comparison of long-run average costs of policies in single relay-node network ($c_t = 1$ and $T = 1$)

c_h, and the "transmit-all" policy is very effective at higher values of c_h (see Figure 7(b) and Figure 7(c)). Further, when either λ_1 or λ_2 is very large, the overall holding costs are insignificant compared to the transmission costs. Therefore, in such a case (e.g. see Figure 7(d)), there is little difference in the performances of the considered policies.

It is also important to see how effective our policies are in availing network coding opportunities. We measure this performance by the "coding ratio" which we define

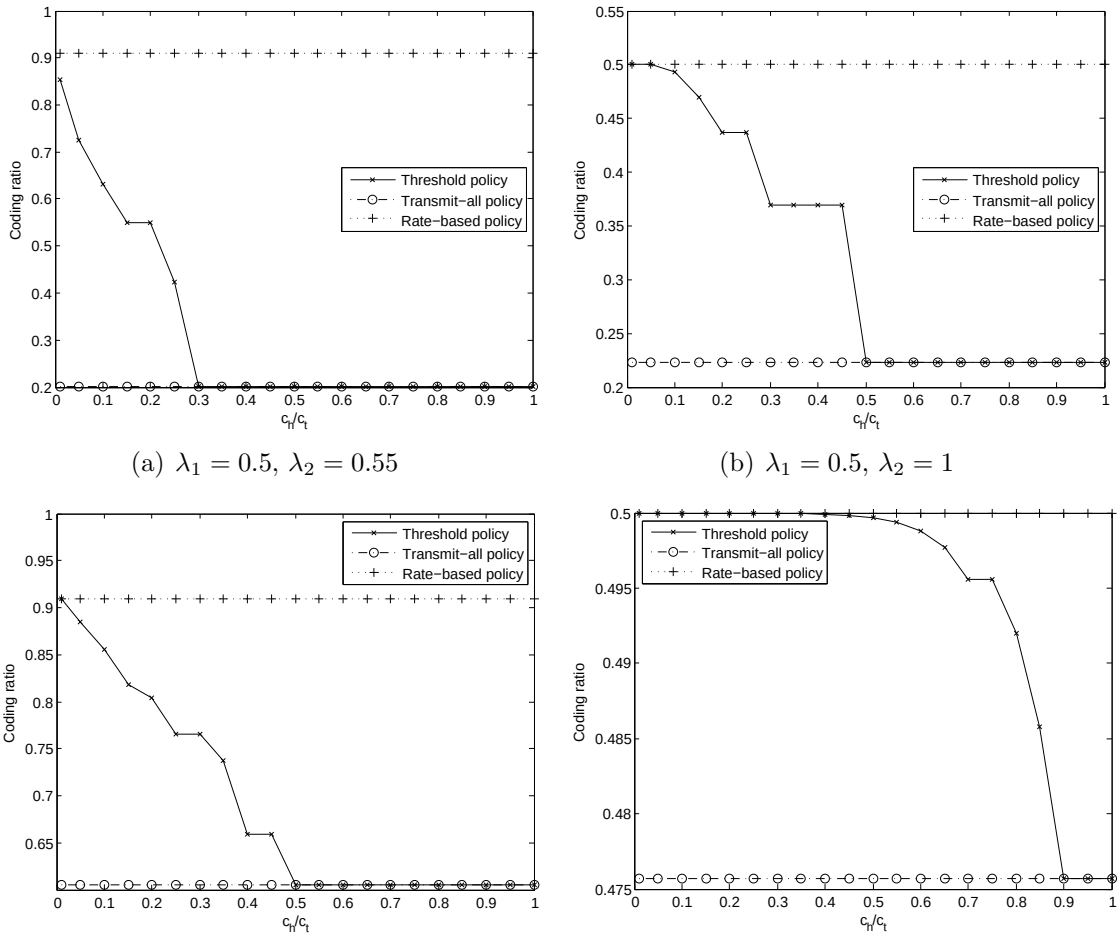

(a) $\lambda_1 = 0.5$, $\lambda_2 = 0.55$ (b) $\lambda_1 = 0.5$, $\lambda_2 = 1$

(c) $\lambda_1 = 5$, $\lambda_2 = 5.5$ (d) $\lambda_1 = 5$, $\lambda_2 = 10$

Figure 8: Comparison of coding ratios of policies in single relay-node network ($c_t = 1$ and $T = 1$)

as the long-run proportion of coded packets in the total number packet transmissions. Figure 8 presents comparison of the coding ratios attained by our policies over different possible values of c_h/c_t in a single relay node network. Notice that the coding ratio of the threshold policy always lies between the coding ratios of the "transmit-all" and "rate-based" policies. The "transmit-all" policy has the lowest coding ratio since it never holds packets for possible network coding opportunities. In case of "rate-based" policy, if $\lambda_1 < \lambda_2$, the total number of coded packets over

the long-run is equal to the total number of packet arrivals to Q_1. Also, the total number of packet transmissions is equal to the total number of packet arrivals to Q_2. Hence the coding ratio in this case is expected to be λ_1/λ_2, which can be observed in Figure 8. Similarly, if $\lambda_1 > \lambda_2$, the coding ratio in the "rate-based" policy will again be a constant and is equal to λ_2/λ_1. It is also important to note that any other policy that tries to achieve a coding ratio higher than the "rate-based" policy will make the system unstable by building up at least one of the queues.

Finally, to study the performance of our policies at a network level, we used them separately in a 4-node line network (see Figure 5(b)). In this case, packets in the input flows f_1 and f_2 (to Q_1 of node 1, and Q_2 of node 4 respectively) arrive as per independent Poisson processes with mean rates λ_1 and λ_2 respectively. Note that the mean rates of packet arrivals to Q_1 and Q_2 of each node are also λ_1 and λ_2 respectively. However, the corresponding arrival processes (except for Q_1 of node 1, and Q_2 of node 4) are not Poisson anymore. Now we consider a transmission schedule in which nodes 1 and 3 transmit together during a transmission opportunity, nodes 2 and 4 transmit together during the next opportunity, and this cycle repeats. In this case, if the time period between consecutive transmission opportunities is T for the network, the corresponding time period for an individual node is $2T$. Therefore the holding cost quantity is $2c_h$ for each node. In this network setup, Figure 9 presents comparison of the long-run average costs of our considered policies at the network level when they are used locally at each node of the network. Notice that the threshold policy achieves the minimum average cost among the considered policies in most cases. Further, the 'transmit-all" and "rate-based" policies perform as good as the threshold policy in specific situations, and these observations are similar to those we discussed in the single node network case. Notice that the effect of holding cost quantity c_h on the average cost is significantly more in the network level compared

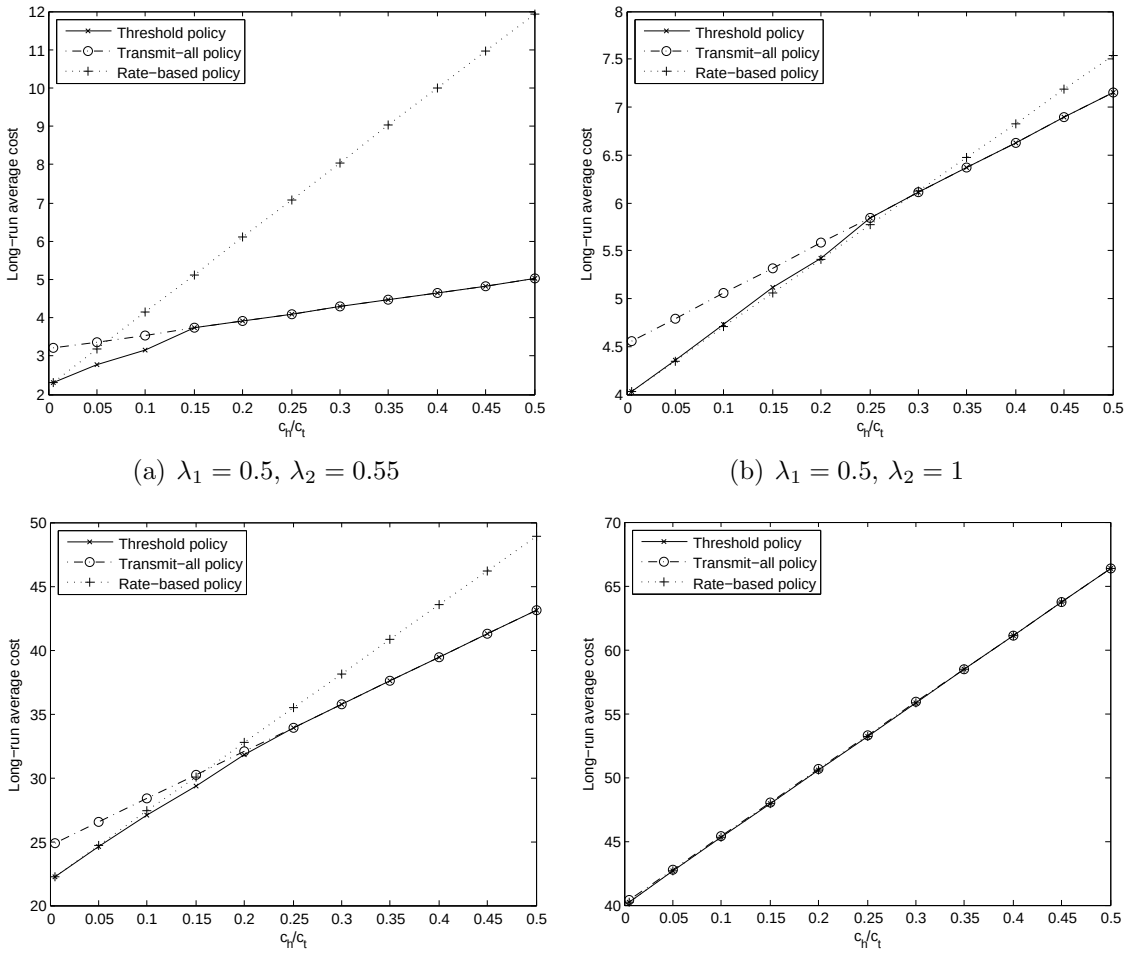

(a) $\lambda_1 = 0.5$, $\lambda_2 = 0.55$

(b) $\lambda_1 = 0.5$, $\lambda_2 = 1$

(c) $\lambda_1 = 5$, $\lambda_2 = 5.5$

(d) $\lambda_1 = 5$, $\lambda_2 = 10$

Figure 9: Comparison of long-run average costs of policies in 4-node line network ($c_t = 1$ and $T = 1$)

to the single node case (see Figure 7). This is primarily because the proportion of the holding costs in the total costs is more in the network level in our considered network case compared to the single node case.

III.7 Conclusion

In this chapter, we developed an MDP based model to manage energy-delay trade-off in network coding decisions in a two-way relay network. We proved that an

optimal stationary policy exists in our average cost MDP. But computing this policy is difficult due to countable number of states in the MDP. However, we showed that, in a certain case, an optimal stationary policy in our MDP is a special type of threshold-based policy. We developed a method to compute this threshold policy. We also found such threshold policy to be very effective in other possible cases. Further, based on the structure of the threshold policy, we developed insights into other simple policies that we showed to be efficient in particular situations.

As our numerical results indicate, the threshold policy performs the best among our considered policies in all situations. However, the "transmit-all" and "rate-based" policies perform as good as the threshold policy in certain situations. These policies are also attractive due to their simplicity and ease in implementation. The "transmit-all" policy is mostly effective when the difference between the mean arrival rates λ_1 and λ_2 is small, and the "rate-based" policy is effective when this difference is considerably large. In other cases of λ_1 and λ_2, the "rate-based" policy performs well when the holding cost c_h is very small compared to the transmission cost c_t, and the "transmit-all" policy performs very well at higher values of c_h.

Many extensions of this work can be considered for future research. The time period T between consecutive transmission opportunities can be considered as a random variable. It would be also worthwhile to see if our results can be extended to the case of a relay that serves as a connection between multiple pairs of nodes. Finally, more effective distributed policies can be explored for managing the energy-delay trade-off in network coding in large wireless networks.

CHAPTER IV

CASE III: AVAILABILITY OF ENERGY HARVESTING SENSOR NODES

IV.1 Introduction

Recent advances in sensor technologies have enabled sensors with renewable energy sources to be used in various applications. In particular, autonomous wireless sensor networks with energy harvesting sensor nodes are gaining prominence in long-lived remote surveillance applications (Kansal *et al.* [32], Kansal and Srivastava [33], Raghunathan *et al.* [57]). These sensors are capable of harvesting energy (such as solar, thermal, vibrational) from the environment. However, in most cases, the rate of energy harvesting is limited. Further, the flow of harvested energy is not fixed and is dependent on the condition of the environment. In fact, in certain environmental conditions, energy generation may not be possible at all. When the energy supply to the sensor is insufficient or unavailable, it is forced to be powered off. The performance of the sensor network is affected when one or more sensor nodes in the network are powered off. Therefore the availability (i.e. proportion of the time that the sensor spends in the ON state with respect to the total time) of the sensor nodes is an important factor in the design and operation of energy harvesting sensor networks. Our objective in this chapter is to evaluate and analyze the long-run availability (also called "limiting availability") of the sensor nodes in such networks.

In an energy harvesting sensor network, every sensor must balance its energy consumption against the amount of energy generated. This is known as "energy-neutral operation" (Kansal *et al.* [32]). In most applications, this is achieved by switching off the sensors from time to time using a node activation policy or schedule.

Note that the sensors consume a negligible amount of energy in the OFF state; however they are still capable of harvesting energy. Under *free operation* (i.e. when no activation policy or schedule is used), a sensor will be ON when it has sufficient energy supply and will be considered OFF otherwise. In this case, the limiting availability of the sensor is the limiting probability of the sensor having a positive energy level. However, the availability of the sensor under a node activation policy will depend on the structure of the activation policy. In this chapter, we develop a model to evaluate the limiting availability of the sensor under a threshold-based node activation policy which has several advantages over free operation.

Recall that the average energy generation rate of an energy harvesting sensor is usually less than its energy consumption rate. Hence, in the long-run, the availability of this sensor (under free operation or any node activation policy) is strictly less than 1. Further, it may not be possible to achieve a desired level of availability with only one sensor node. In such a case, it is appropriate to use a multi-sensor system where it is sufficient to keep only one sensor ON at any time while the remaining "backup" sensors are OFF. However, the question arises how many sensors are required in this system and how they will be operated to achieve the required level of availability. We aim to develop analytical models to compute and analyze the combined availability in such multi-sensor systems.

The remainder of this chapter is organized as follows. We present a review of important related works in Section IV.2. In Section IV.3, we model the energy flow in an energy harvesting sensor as a stochastic fluid-flow queue. In Section IV.4, we develop an approach to compute the limiting availability of an energy harvesting sensor under threshold-based node-activation policy. In Sections IV.5 and IV.6, we consider limiting availability of multi-sensor systems. Finally, in Section IV.7, we present our concluding remarks and outline some future research directions.

IV.2 Literature Review

In recent years, there has been an increasing interest in the research community in energy management policies for energy harvesting wireless sensor networks. Kansal *et al.* [32] introduced various energy management techniques to ensure energy-neutral operation in such networks. Sharma *et al.* [68] proposed a throughput-optimal energy management policy for a single energy harvesting node. Srivastava *et al.* [71] focused on analyzing the node-level performance in such a policy. Jaggi *et al.* [29] and Kar *et al.* [34] considered utility of an energy harvesting sensor network with continuous charging. They considered a different kind of threshold policy which tries to keep a fixed number of sensors in the ON state. The availability measure has not been considered for any similar system. However, various models exist in the reliability and maintenance literature (e.g. see works by Kharoufeh *et al.* [36] and Kiessler *et al.* [38]) to compute the availability of different maintainable systems.

In this chapter, we model the energy flow in an energy harvesting sensor as a stochastic fluid-flow queue. Jones *et al.* [30] used a similar fluid queue model for a rechargeable battery. They computed the battery life period from fully charged state to no-charge state while considering two different energy discharge rates. There are also various fluid-flow models available in the literature for different applications. In particular, there has been a lot of interest in such models for telecommunication applications since the seminal work by Anick *et al.* [7]. However, most of the works in this area have so far focused on the steady-state analysis of the buffer content process. There are a few important works on first passage times which we use in our analyses. Narayanan and Kulkarni [53] developed general expressions for first passage times in a stochastic fluid-flow queue where the input flow rate is controlled by a continuous-time Markov chain. Kulkarni and Tzenova [43] developed a method

for directly calculating the mean first passage times in such a system. Using a similar fluid-flow model, Kharoufeh and Gautam [37] derived analytical expressions for travel time distribution for a vehicle traversing a freeway link of arbitrary length. Recent works in this area (e.g. Ahn and Ramaswamy [3], Barbot *et al.* [11], Es-Saghouani and Mandjes [21]) have focused on developing methods to compute the busy period distribution in stochastic fluid-flow models. Various performance measures of fluid flow queueing systems under different operating policies have also been studied in the literature. In different problem setups, Aggarwal *et al.* [1], Baek *et al.* [10], and Mahabhashyam *et al.* [48] have analyzed the performance of threshold-based policies in such systems.

IV.3 Fluid-flow Model of an Energy Harvesting Sensor

We model the energy flow in an energy harvesting sensor as a stochastic fluid-flow queue as shown in Figure 10. The environment (which acts as the energy source) is described by an irreducible continuous-time Markov chain $\{Z(t), t \geq 0\}$ with a finite state space $\mathcal{S} = \{1, \ldots, M\}$, infinitesimal generator $\boldsymbol{Q} = [q_{ij}]$, and stationary distribution $\boldsymbol{\pi}$. We assume that the environment is stationary in the beginning, i.e. the distribution of $Z(0)$ is $\boldsymbol{\pi}$. When the environment is in state $i \in \mathcal{S}$, energy flows into the sensor at a rate $r_i \geq 0$. The maximum amount of energy that can be stored in the sensor is K (which can also be ∞). The rate of energy consumption of the sensor is fixed and is denoted by c. For ease in exposition, we assume that $r_i - c \neq 0$

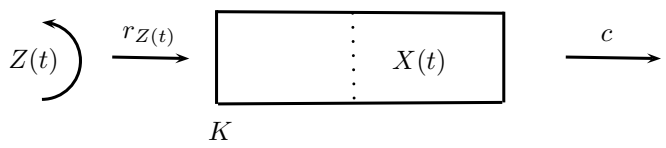

Figure 10: Fluid-flow model of an energy harvesting sensor

for all $i \in \mathcal{S}$. However, a model without this assumption is still analytically tractable. We also assume $\sum_{i\in\mathcal{S}} \pi_i r_i < c$ since the average recharge rate of a sensor is typically lower than the average discharge rate in energy harvesting sensor networks (Jaggi *et al.* [29]). For this reason, each sensor is forced to be in the OFF state from time to time to operate in an energy-neutral manner.

Suppose $X(t)$ is the amount of energy available in the sensor at time t. Under free operation of the sensor, the dynamics of $\{X(t), t \geq 0\}$ are described by

$$\frac{dX(t)}{dt} = \begin{cases} r_{Z(t)} - c & \text{if } X(t) > 0, \\ \max(r_{Z(t)} - c, 0) & \text{if } X(t) = 0, \\ \min(r_{Z(t)} - c, 0) & \text{if } X(t) = K. \end{cases} \tag{53}$$

This is a Markov fluid-flow model where $\{(X(t), Z(t)), t \geq 0\}$ is a Markov process (Kulkarni [42]). When $K = \infty$, this process is stable under the condition $\sum_{i\in\mathcal{S}} \pi_i r_i < c$, which holds in our application. Under free operation, the sensor is ON when $X(t) > 0$, and is considered to be OFF when $X(t) = 0$. Hence, in this case, the limiting availability of the sensor is $\bar{A} = \lim_{t\to\infty} \mathrm{P}(X(t) > 0)$, which can be computed from the limiting distribution of $\{(X(t), Z(t)), t \geq 0\}$ process (Gautam [22]).

In the free operation, observe from (53) that the input energy is actually wasted in two cases: (1) when $X(t) = K$ and $r_{Z(t)} > c$, and (2) when $X(t) = 0$ and $r_{Z(t)} < c$. In the first case, energy loss can be reduced by selecting the energy capacity K as large as possible (this loss is avoided if $K = \infty$). The energy loss in the second case is entirely avoidable through node activation policies that allow the input energy to be stored in such situation by switching off the sensor for certain time period. In the following section, we consider a threshold-based node activation policy which has several advantages over free operation.

IV.4 Availability of a Single Sensor Node Under Threshold-based Activation Policy

Under a threshold-based node activation policy, a sensor is switched on when its energy level rises to a fixed threshold level L ($< K$) and is switched off when its energy level falls to zero. When a proper threshold level L is set, this policy will lead to less frequent on-off cycles compared to the free operation. Further, L can be set to ensure (with certain probability) an ON time period long enough to detect a series of events. Now we will develop an approach to compute the limiting availability of a sensor node under threshold-based activation policy.

In one of the important related works, Kiessler *et al.* [38] developed an approach to compute the limiting average availability of a periodically inspected system subject to Markovian degradation. The idea of limiting availability in our formulation in this section is essentially derived from their work. However, the energy level in our considered system can go up and down, thereby requiring a different analysis. Also, we find the limiting availability in our case instead of limiting average availability. Further, we use a different approach based on first passage time analysis to compute the limiting availability. In fact, the methods used by Kiessler *et al.* [38] and Kharoufeh *et al.* [36] in their problems will not work in our case.

Now let $X(t)$ be the amount of energy in the sensor at time t under the threshold-based policy. The state of the sensor is described by $Y(t)$, which is equal to 1 if the sensor is ON at time t, else is 0. In this case, the dynamics of the energy flow in the sensor are described by

$$\frac{dX(t)}{dt} = r_{Z(t)} - cY(t).$$

Figure 11 shows a sample path of $X(t)$ over one on-off cycle of the sensor. Let U_n and D_n denote the ON and OFF time periods of the sensor during the n-th

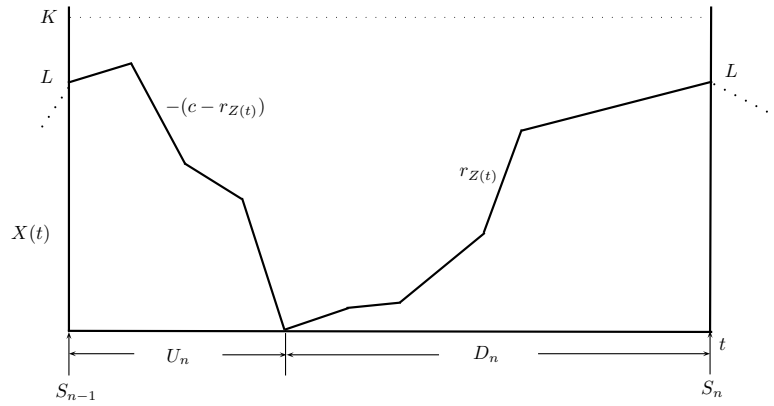

Figure 11: Sample path of $X(t)$ under threshold-based node activation policy

cycle. Let S_n denote the end time of the n-th cycle with $S_0 = 0$. We also define $\xi_n = Z(S_n)$, which is the state of the environment at S_n. It can be shown that the process $\{\xi_n, n \geq 0\}$ is an irreducible discrete-time Markov chain. We denote its transition probability matrix and stationary distribution by $\hat{\boldsymbol{P}}$ and $\hat{\boldsymbol{\pi}}$ respectively (though they are yet to be determined). Now we present the main results of this section in Theorems 3 and 4.

Theorem 3. *The sequence* $\{(\xi_n, S_n), n \geq 0\}$ *is a Markov renewal sequence, and the process* $\{Y(t), t \geq 0\}$ *is Markov regenerative with respect to this Markov renewal sequence.*

Proof. Note that the random variables $\{S_n, n \geq 0\}$ are stopping times with respect to the history generated by the environment process $\{Z(t), t \geq 0\}$. Hence the strong Markov property holds at these times. Therefore, for all $n \geq 0$, we have

$$\begin{aligned}
&\mathrm{P}\{\xi_{n+1} = j, S_{n+1} - S_n \leq t |\ \xi_n = i, S_n, \xi_{n-1}, S_{n-1}, \ldots, \xi_0, S_0\} \\
&= \mathrm{P}\{\xi_{n+1} = j, S_{n+1} - S_n \leq t |\ \xi_n = i\} \\
&= \mathrm{P}\{\xi_1 = j, S_1 \leq t |\ \xi_0 = i\},
\end{aligned}$$

which shows that $\{(\xi_n, S_n), n \geq 0\}$ is a Markov renewal sequence (Kulkarni [41]). Also, the conditional distribution of $\{Y(S_n+t), t \geq 0\}$ given $\{Y(s), 0 \leq s \leq S_n, \xi_n = i\}$ is same as that of $\{Y(t), t \geq 0\}$ given $\xi_0 = i$. Therefore $\{Y(t), t \geq 0\}$ is Markov regenerative with respect to the Markov renewal sequence $\{(\xi_n, S_n), n \geq 0\}$. □

Theorem 4. *The limiting availability $\bar{A}$ of the sensor under threshold-based node activation policy is given by*

$$\bar{A} = \lim_{t\to\infty} \frac{\int_0^t Y(w)\ dw}{t} = \frac{\sum_{i\in\mathcal{S}} \hat{\pi}_i\ E[U_1|\xi_0 = i]}{\sum_{i\in\mathcal{S}} \hat{\pi}_i\ E[S_1|\xi_0 = i]}. \tag{54}$$

Proof. Suppose $\xi_0 = j$ for some $j \in \mathcal{S}$. Let $\{S_n^j, n \geq 0\}$ be the sequence of consecutive S_n at which $\xi_n = j$. Note that $\{S_n^j, n \geq 0\}$ is a renewal sequence with $S_0^j = 0$. Using a renewal reward process argument (Resnick [58]), we have

$$\bar{A} = \lim_{t\to\infty} \frac{\int_0^t Y(w)\ dw}{t} = \frac{\mathrm{E}[\int_0^{S_1^j} Y(w)\ dw]}{\mathrm{E}[S_1^j]}. \tag{55}$$

Now, using Theorem 3, it can be shown that (see proof of Theorem 2 in Kiessler *et al.* [38])

$$\mathrm{E}[\textstyle\int_0^{S_1^j} Y(w)\ dw] = \displaystyle\sum_{i\in\mathcal{S}} \frac{\hat{\pi}_i}{\hat{\pi}_j}\ \mathrm{E}[U_1|\xi_0 = i], \tag{56}$$

$$\mathrm{E}[S_1^j] = \sum_{i\in\mathcal{S}} \frac{\hat{\pi}_i}{\hat{\pi}_j}\ \mathrm{E}[S_1|\xi_0 = i]. \tag{57}$$

Now, using the results (56) and (57) in (55), we have

$$\bar{A} = \frac{\sum_{i\in\mathcal{S}}(\hat{\pi}_i/\hat{\pi}_j)\ \mathrm{E}[U_1|\xi_0 = i]}{\sum_{i\in\mathcal{S}}(\hat{\pi}_i/\hat{\pi}_j)\ \mathrm{E}[S_1|\xi_0 = i]} = \frac{\sum_{i\in\mathcal{S}} \hat{\pi}_i\ \mathrm{E}[U_1|\xi_0 = i]}{\sum_{i\in\mathcal{S}} \hat{\pi}_i\ \mathrm{E}[S_1|\xi_0 = i]},$$

which proves the result in (54). □

IV.4.1 Computation of Limiting Availability

To compute the limiting availability given in (54), we need to find the conditional expectations $\mathrm{E}[U_1|\xi_0 = i]$ and $\mathrm{E}[S_1|\xi_0 = i]$ for all $i \in \mathcal{S}$, and also the stationary distribution $\hat{\boldsymbol{\pi}}$ of the Markov chain $\{\xi_n, n \geq 0\}$. In the following subsections, we present our approach to compute these quantities.

IV.4.1.1 Distribution of U_1

When the sensor node is in the ON state, we define the first passage time to the OFF state as $U := \inf\{t > 0 : X(t) = 0\}$. Now consider the joint distribution

$$H_{ij}^U(x,t) = \mathrm{P}\{U \leq t, Z(U) = j | X(0) = x, Z(0) = i\}$$

for $i, j \in \mathcal{S}, x \geq 0$ and $t \geq 0$. Our objective here is to compute $H_{ij}^U(L,t)$ which is precisely the conditional distribution of U_1, defined as $G_{ij}^{U_1}(t) = \mathrm{P}(U_1 \leq t, Z(U_1) = j|\xi_0 = i)$. The distribution $\boldsymbol{H}^U(x,t) = [H_{ij}^U(x,t)]$ is known to satisfy the following partial differential equation (Gautam [22]).

$$\frac{\partial \boldsymbol{H}^U(x,t)}{\partial t} - \boldsymbol{D}\frac{\partial \boldsymbol{H}^U(x,t)}{\partial x} = \boldsymbol{Q}\boldsymbol{H}^U(x,t), \tag{58}$$

where $\boldsymbol{D}$ is a diagonal matrix with $[\boldsymbol{D}]_{ii} = r_i - c$ for $i = 1, \ldots, |\mathcal{S}|$. At the first passage time U, the environment cannot be in a state j with $r_j > c$. Hence $H_{ij}^U(x,t) = 0$ for all j with $r_j > c$. Moreover, the following boundary conditions hold for $H_{ij}^U(x,t)$.

$$H_{ij}^U(0,t) = 1 \quad \text{if } i = j \text{ and } r_i < c, \tag{59}$$

$$H_{ij}^U(0,t) = 0 \quad \text{if } i \neq j \text{ and } r_i < c. \tag{60}$$

Taking the Laplace-Stieltjes Transform (LST) on both sides of (58) with respect to t, we obtain the following ordinary differential equation (ODE).

$$\boldsymbol{D}\frac{d\tilde{\boldsymbol{H}}^{U}(x,w)}{dx} = (w\boldsymbol{I} - \boldsymbol{Q})\tilde{\boldsymbol{H}}^{U}(x,w), \tag{61}$$

where $\tilde{\boldsymbol{H}}^{U}(x,w) = [\tilde{H}^{U}_{ij}(x,w)]$ and $\tilde{H}^{U}_{ij}(x,w) = \int_0^\infty e^{-wt}\, dH^{U}_{ij}(x,t)$. The differential equations (58) and (61) hold in both finite and infinite energy storage capacity cases. However, in the finite capacity case (i.e. $K < \infty$), if the energy level reaches K in a state i (which will happen if $r_i > c$), it will stay there until the environment changes to some other state k. This leads to an additional condition which we can write in the LST domain as

$$\tilde{H}^{U}_{ij}(K,w) = \sum_{k\neq i} \frac{q_{ik}}{-q_{ii}+w}\tilde{H}^{U}_{kj}(K,w). \tag{62}$$

To solve the ODE (61), we use the *spectral decomposition* technique (Gautam [22]) which provides the solution in the following form.

$$\begin{pmatrix} \tilde{H}^{U}_{1j}(x,w) \\ \vdots \\ \tilde{H}^{U}_{|\mathcal{S}|j}(x,w) \end{pmatrix} = \sum_{i=1}^{|\mathcal{S}|} a_{ij}(w)e^{s_i(w)x}\boldsymbol{\phi}_i(w), \quad j \in \mathcal{S}, \tag{63}$$

where $a_{ij}(w)$ are unknown coefficients (to be found using boundary conditions (59)-(60) and (62)), and $s_i(w)$ and $\boldsymbol{\phi}_i(w)$ are the eigenvalues and eigenvectors satisfying the equations $s_i(w)\boldsymbol{D}\boldsymbol{\phi}_i(w) = (w\boldsymbol{I} - \boldsymbol{Q})\boldsymbol{\phi}_i(w)$ for $i \in \mathcal{S}$.

Once $\tilde{\boldsymbol{H}}^{U}(x,w)$ is determined, we can find the LST of the conditional distribution of U_1 as $\tilde{G}^{U_1}_{ij}(w) = \tilde{H}^{U}_{ij}(L,w)$. Also, we can compute the required conditional

expectation $\mathrm{E}[U_1|\xi_0 = i]$ in the following way.

$$\mathrm{E}[U_1|\xi_0 = i] = -\frac{d}{dw}\sum_{j\in\mathcal{S}} \tilde{H}^U_{ij}(L, w) \quad \text{at } w = 0.$$

IV.4.1.2 Distribution of S_1

To compute the distribution of S_1, we will first compute the distribution of D_1. When the sensor node is in the OFF state, we define the first passage time to the ON state as $D := \inf\{t > 0 : X(t) = L\}$. Now consider the joint distribution

$$H^D_{ij}(x, t) = \mathrm{P}\{D \le t, Z(D) = j|X(0) = x, Z(0) = i\}$$

for $i, j \in \mathcal{S}, x \ge 0, t \ge 0$. Our objective here is to compute $H^D_{ij}(0, t)$ which is same as the conditional distribution of D_1, defined as $G^{D_1}_{ij}(t) = \mathrm{P}(S_1 - U_1 \le t, Z(S_1) = j|Z(U_1) = i) = \mathrm{P}\{D_1 \le t, Z(D_1) = j|Z(0) = i\}$ (by the strong Markov property at U_1). The distribution $\boldsymbol{H}^D(x, t) = [H^D_{ij}(x, t)]$ satisfies the following partial differential equation.

$$\frac{\partial \boldsymbol{H}^D(x, t)}{\partial t} - \boldsymbol{R}\frac{\partial \boldsymbol{H}^D(x, t)}{\partial x} = \boldsymbol{Q}\boldsymbol{H}^D(x, t), \tag{64}$$

where $\boldsymbol{R}$ is a diagonal matrix with $[\boldsymbol{R}]_{ii} = r_i$ for $i = 1, \ldots, |\mathcal{S}|$. The following boundary conditions hold for $H^D_{ij}(x, t)$.

$$H^D_{ij}(L, t) = 1 \quad \text{if } i = j \text{ and } r_i > 0, \tag{65}$$

$$H^D_{ij}(L, t) = 0 \quad \text{if } i \ne j \text{ and } r_i > 0. \tag{66}$$

By taking the LST on both sides of (64) with respect to t, we obtain

$$\boldsymbol{R}\frac{d\tilde{\boldsymbol{H}}^{D}(x,w)}{dx} = (w\boldsymbol{I} - \boldsymbol{Q})\tilde{\boldsymbol{H}}^{D}(x,w), \tag{67}$$

where $\tilde{\boldsymbol{H}}^{D}(x,w) = [\tilde{H}_{ij}^{D}(x,w)]$ and $\tilde{H}_{ij}^{D}(x,w) := \int_0^\infty e^{-wt}\ dH_{ij}^{D}(x,t)$. As in the previous subsection, we can solve the differential equation (67) using the spectral decomposition technique where the solution is of the same format as in (63). However, in this case, the boundary conditions in (65)-(66) may not be always sufficient to find all the unknown coefficients $a_{ij}(w)$ in (63). There we need to use additional conditions including $a_{ij}(w) = 0$ if $s_i(w) > 0$ (Narayanan and Kulkarni [53]).

Once $\tilde{\boldsymbol{H}}^{D}(x,w)$ is determined, we can find the LST of the conditional distribution of D_1 as $\tilde{G}_{ij}^{D_1}(w) = \tilde{H}_{ij}^{D}(0,w)$. Now the following theorem provides the conditional distribution of S_1, which we define as $G_{ij}^{S_1}(t) = \mathrm{P}(S_1 \le t, Z(S_1) = j | \xi_0 = i)$.

Theorem 5. *$\tilde{\boldsymbol{G}}^{S_1}(w) = \tilde{\boldsymbol{G}}^{U_1}(w)\ \tilde{\boldsymbol{G}}^{D_1}(w)$, where $\tilde{\boldsymbol{G}}^{(\cdot)}(w) = [\tilde{G}_{ij}^{(\cdot)}(w)]$.*

Proof. Since the strong Markov property holds at time U_1, we show that

$$\begin{aligned}
G_{ij}^{S_1}(t) &= \mathrm{P}\{S_1 \le t, Z(S_1) = j | Z(0) = i\} \\
&= \sum_k \int_o^s \mathrm{P}\{S_1 \le t, Z(S_1) = j | Z(0) = i, Z(U_1) = k, U_1 = s\}\ dG_{ik}^{U_1}(s) \\
&= \sum_k \int_o^s \mathrm{P}\{S_1 - U_1 \le t - s, Z(S_1) = j | Z(U_1) = k\}\ dG_{ik}^{U_1}(s) \\
&= \sum_k \int_o^s \mathrm{P}\{D_1 \le t - s, Z(D_1) = j | Z(0) = k\}\ dG_{ik}^{U_1}(s) \\
&= \sum_k \int_o^s G_{kj}^{D_1}(t - s)\ dG_{ik}^{U_1}(s) \\
&= [\boldsymbol{G}^{U_1} * \boldsymbol{G}^{D_1}(t)]_{ij}.
\end{aligned} \tag{68}$$

The result follows when LST is taken on both sides of (68). □

Now we can compute the required conditional expectation $\mathrm{E}[S_1|\xi_0 = i]$ in the following way.

$$\mathrm{E}[S_1|\xi_0 = i] = -\frac{d}{dw}\sum_{j\in\mathcal{S}} \tilde{G}_{ij}^{S_1}(w) \quad \text{at } w = 0.$$

Further, note that the transition probability matrix of the Markov chain $\{\xi_n, n \geq 0\}$ is $\hat{\boldsymbol{P}} = \boldsymbol{G}^{S_1}(\infty) = \tilde{\boldsymbol{G}}^{S_1}(0)$. Therefore the stationary distribution $\hat{\boldsymbol{\pi}}$ of this Markov chain can be found by solving the equations $\hat{\boldsymbol{\pi}} = \hat{\boldsymbol{\pi}}\tilde{\boldsymbol{G}}^{S_1}(0)$ and $\sum_{i\in\mathcal{S}} \hat{\pi}_i = 1$.

IV.4.2 Special Case: Exponential On-Off Environment

Consider an alternating exponential on-off process for the environment which acts as the energy source. In this case, the environment is described by a continuous-time Markov chain with state space $\{0, 1\}$ and infinitesimal generator matrix

$$\boldsymbol{Q} = \begin{bmatrix} -\beta & \beta \\ \alpha & -\alpha \end{bmatrix}.$$

Energy flows into the sensor at rate r when the environment is in state 1, and at rate 0 when the environment is in state 0. Since the average recharge rate of the sensor is usually lower than its average discharge rate, we assume $\frac{r\beta}{\alpha+\beta} < c$.

Figure 12 shows a sample path of the sensor energy level $X(t)$ during one on-off cycle of the sensor when a threshold-based activation policy is used. Here an on-off cycle of the sensor will always begin in the environment state 1. Therefore, in this case, $\{Y(t), t \geq 0\}$ is a regenerative process, and the limiting availability of the sensor is given by (Resnick [58]):

$$\bar{A} = \lim_{t\to\infty} \frac{\int_0^t Y(w)\ dw}{t} = \frac{\mathrm{E}[U_1]}{\mathrm{E}[S_1]}, \tag{69}$$

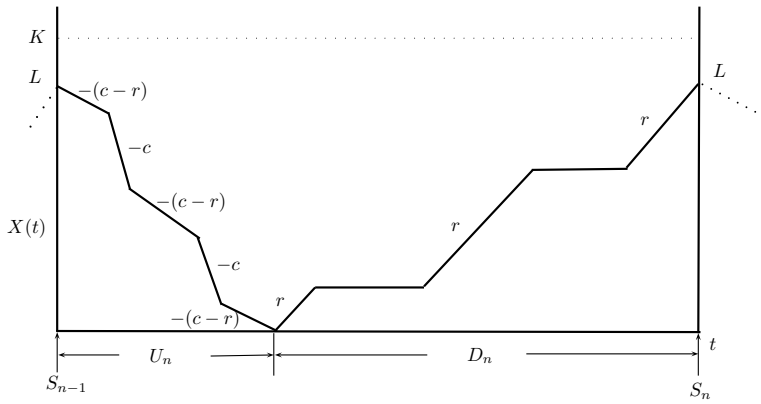

Figure 12: Sample path of $X(t)$ in an exponential on-off environment

which is a special case of the expression in (54). To find the availability $\bar{A}$ in (69), the quantities $\mathrm{E}[U_1]$ and $\mathrm{E}[S_1]$ can be computed using our approach described in the previous subsection.

IV.4.3 Numerical Example

In this subsection, we demonstrate the computation of limiting availability of a sensor node. All computations in the presented example were performed in MATLAB, and we used numerical procedure for differentiation.

We consider a sensor node with energy storage capacity of $K = 50$. The environment is described by a continuous-time Markov chain with state space $\{1, 2, 3, 4, 5\}$ and infinitesimal generator matrix given by

$$\boldsymbol{Q} = \begin{bmatrix} -1 & 0.4 & 0.3 & 0.2 & 0.1 \\ 0.4 & -0.7 & 0.1 & 0.1 & 0.1 \\ 0.5 & 0.4 & -1.1 & 0.1 & 0.1 \\ 0.2 & 0.3 & 0.3 & -1 & 0.2 \\ 0.3 & 0.3 & 0.3 & 0.3 & -1.2 \end{bmatrix}.$$

Table 3: Computed conditional means and stationary probabilities

i	$\mathrm{E}[U_1\|\xi_0 = i]$	$\mathrm{E}[S_1\|\xi_0 = i]$	$\hat{\pi}_i$
1	13.6790	20.2584	0.0767
2	13.5887	20.1682	0.1938
3	15.6396	22.2190	0.2790
4	16.7978	23.3772	0.2569
5	16.8318	23.4112	0.1937

The energy inflow rates in environment states 1 to 5 are given by the vector $\boldsymbol{r} = [2, 4, 12, 14, 16]$. The energy consumption rate of the sensor is $c = 10$. A threshold level $L = 40$ is considered in the threshold-based activation policy.

Using our approach described in Section IV.4.1, the conditional means $\mathrm{E}[U_1|\xi_0 = i]$ and $\mathrm{E}[S_1|\xi_0 = i]$, and the stationary probabilities $\hat{\pi}_i$ are calculated and are shown in Table 3. Now, using (54), the limiting availability is found as

$$\bar{A} = \frac{\sum_{i=1}^{5} \hat{\pi}_i \, \mathrm{E}[U_1|\xi_0 = i]}{\sum_{i=1}^{5} \hat{\pi}_i \, \mathrm{E}[S_1|\xi_0 = i]} = 0.7036.$$

We repeated our computations for different values of the threshold L between 0 and $K = 50$. For these values of L, we also computed the limiting availability in the case $K = \infty$. Figure 13 shows how the limiting availability of the sensor changes over the range of L in the cases $K = 50$ and $K = \infty$. Observe that, in the finite capacity case $K = 50$, the limiting availability decreases as the threshold L increases towards K. This is because energy loss due to overflow increases (hence less amount of energy is available to the sensor) at higher values of L. However, note that such energy loss does not occur in the case $K = \infty$. In this case, the sensor receives energy at an average rate $\sum_{i=1}^{5} \pi_i r_i$, where $\boldsymbol{\pi}$ is the stationary distribution of the environment process and is found to be $\boldsymbol{\pi} = [0.2725, 0.3438, 0.1652, 0.1315, 0.0870]$. Since the

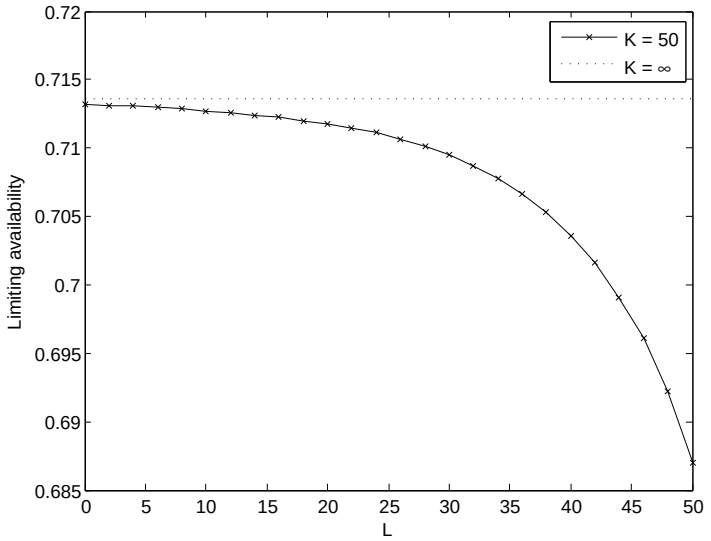

Figure 13: Limiting availability for different values of threshold (L)

sensor consumes energy at rate c during ON periods, the limiting availability is expected to be $\sum_{i=1}^{5} \pi_i r_i / c = 0.7136$ (based on energy flow balance). Note that the availability in this case is independent of the threshold L, which can also be observed in Figure 13.

IV.5 Availability of a Multi-sensor System with Infinite Capacity Sensor Nodes

In this section, we consider availability of an energy harvesting multi-sensor system used for continuous monitoring of events or environmental conditions over an area. In particular, we consider an application where there are N sensors, but only one sensor is ON at a time. In this case, the sensor system is considered to be operational or available if at least one of the sensor nodes is in the ON state. In most of such applications, all sensors receive energy from the same environment (e.g. solar-powered sensors). Hence the energy recharge processes at the sensors are completely correlated. Also, all sensors have the same fixed energy discharge rate. Note that,

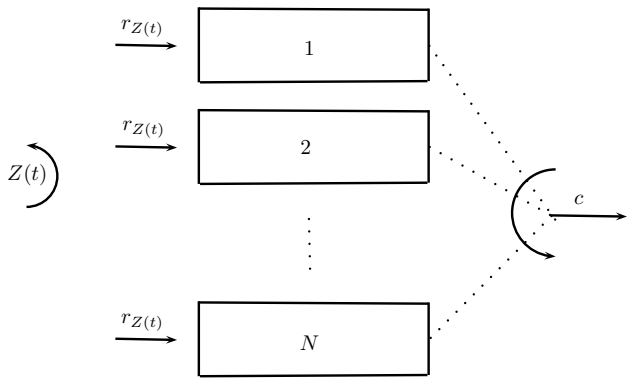

Figure 14: Energy flow model of an energy harvesting multi-sensor system

in this case, if all sensors in the system are deployed at the same time, and each sensor is operated independently under free operation or under an activation policy, the sensors will always turn on or off at the same time. So the combined availability $\bar{A}_{\text{net}}$ of all the sensors at the system level will be the same as the availability of a single sensor node $\bar{A}$. Therefore, the idea is to manage the energy consumption in the sensors in a coordinated manner so that the sensors will have disjoint on-periods, and their individual availability measures will add up at the system level. Based on this idea, we introduce simple policies to operate such a system and analyze its limiting availability $\bar{A}_{\text{net}}$ under these policies.

Figure 14 shows the energy flow model of the considered system with N energy harvesting sensors which receive energy from the same environment. The descriptions of the Markovian environment and stochastic fluid-flow model of the sensor remain the same as in the single sensor case. Note that energy flows into all sensors simultaneously. However, it is sufficient to keep only one sensor ON at any time. Now we introduce the following policies to operate this system.

1. *Exhaustive Service Policy*: In this policy, sensors are switched on in a cyclic order $(1, \ldots, N, 1, \ldots)$. From the time of switching on, a sensor is kept in

the ON state until its energy level reaches zero. It is then switched off and the transition to next sensor is made. Note that this policy is similar to the exhaustive service policy in a polling system (Takagi [73]).

2. *Threshold-based Exhaustive Service Policy*: This policy is similar to the exhaustive service policy. However, upon transition to a particular sensor, if its energy level is found to be is zero (note that energy levels of all other sensors are also zero at this time), it is kept in the OFF state until its energy level reaches a threshold value L. It is then turned on, and regular cyclic service order is followed.

In this section, we consider the case where the sensors have infinite energy storage capacity, i.e. $K = \infty$. To ensure stability, we assume here that the average combined recharge rate is lower than the average discharge rate, i.e. $N \sum_{i \in \mathcal{S}} \pi_i r_i < c$. In this case, suppose $X_k(t)$ is the amount of energy in the k-th sensor ($k = 1, \ldots, N$) at time t under exhaustive service policy. Note that the considered system is available when $X(t) := \sum_{k=1}^{N} X_k(t) > 0$ and is considered to be unavailable when $X(t) = 0$. Thus the limiting availability $\bar{A}_{\text{net}}$ of the system is equal to the limiting availability of an equivalent single sensor node under free operation. Note that energy flows into this single sensor at the rate $Nr_{Z(t)}$, where $Z(t)$ is the state of the environment at time t. Its availability can be computed as discussed in Section IV.3.

Now consider the given system under threshold-based exhaustive service policy with threshold L. In this case, it can be shown that the total energy in the system $X(t) := \sum_{k=1}^{N} X_k(t)$ is equal to the amount of energy in an equivalent single sensor node under threshold activation policy with threshold NL. Therefore, $\bar{A}_{\text{net}}$ of the system is equal to the limiting availability of this single sensor node under threshold-based activation policy, which can be computed as discussed in Section IV.4.

IV.6 A Lower Bound for Availability of a Multi-sensor System with Finite Capacity Sensor Nodes

In the previous section, we introduced an approach to compute the limiting availability of an energy harvesting multi-sensor system (Figure 14) under selected policies when the sensor nodes have infinite energy capacity. It is however difficult to develop tractable methods to compute the availability of such a system when the sensors have finite energy capacity. In this case, knowledge of a good lower bound on system-level availability is useful since it can provide a reasonable estimate of the number of sensors required to achieve a desired level of availability. In this section, we develop a method to compute such a lower bound when an exhaustive service policy is used.

Consider again the multi-sensor system in Figure 14 with N energy harvesting sensor nodes. The energy storage capacity of each sensor is $K < \infty$. Under an exhaustive service policy, let $X(t) := \sum_{k=1}^{N} X_k(t)$ denote the total amount of energy in the system at time t, where $X_k(t)$ is the amount of energy in the k-th sensor $(k = 1, \ldots, N)$ at time t. To find a good lower bound on the availability of this system, we consider a close enough but fictitious system that operates in identical conditions. Let $\bar{X}(t)$ be the total amount of energy in this new system at time t. Here we assume that, when $iK \leq \bar{X}(t) < (i+1)K$ (for $i = 0, \ldots, N-1$), exactly i sensors are full to capacity K. Note that, in this situation in our original system (i.e. when $iK \leq X(t) < (i+1)K$), at most i sensors will be full to capacity. Since the new system rejects more harvested energy than the original system, we have $\bar{X}(t) \leq X(t)$ for $t \geq 0$. Therefore, the availability of the new system is a lower bound on the availability of our original system.

Figure 15 shows the equivalent single sensor model of our new system. In this case, the energy inflow rate at time t is given by $\bar{r}(t) = (N-i+1)r_j$ when $(i-1)K \leq$

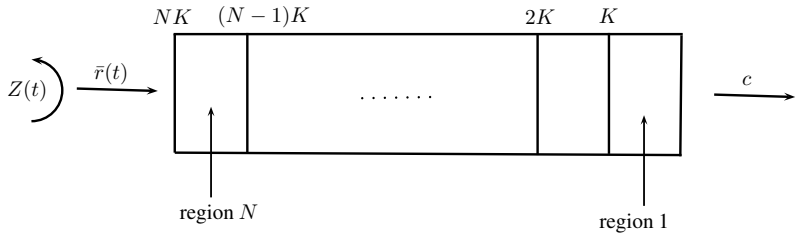

Figure 15: Model for computation of lower bound on system-level availability

$\bar{X}(t) < iK$ (for $i = 1, \ldots, N$), and the state of the environment is $j \in \mathcal{S}$. Here the distinct energy levels $0, K, 2K, \cdots, NK$ are called *thresholds*. When the energy level in the system $\bar{X}(t)$ lies between the thresholds $(i-1)K$ and iK, it is said to be in *region* i $(i = 1, \ldots, N)$.

Note that the energy inflow to the considered system is dependent on the energy level in the system as well as the state of the environment. However, the output rate remains constant at c at all times. When the energy level $\bar{X}(t)$ is in region i and $Z(t) = j$, the energy inflow rate is $(N - i + 1)r_j$. For ease of exposition, we assume that $(N - i + 1)r_j - c \neq 0$ for every $i \in \{1, \ldots, N\}$ and $j \in \mathcal{S}$. Now, for region i, we define the sets of positive drift and negative drift environment states respectively as

$$\begin{aligned} \mathcal{S}_i^+ &= \{j \in \mathcal{S} : (N - i + 1)r_j - c > 0\}, \\ \mathcal{S}_i^- &= \{j \in \mathcal{S} : (N - i + 1)r_j - c < 0\}. \end{aligned}$$

Note that $\bar{X}(t)$ will increase in region i if $Z(t) \in \mathcal{S}_i^+$, and will decrease if $Z(t) \in \mathcal{S}_i^-$. Now, consider a region i and and an environmental state j such that $j \in \mathcal{S}_i^+$, but $j \in \mathcal{S}_{i+1}^-$. In this case, while the environment remains in state j, the energy level in the system will cross the threshold iK from below and enter region i+1. At this point, if the environment continues to be in state j, the energy level will instantaneously

cross threshold iK from above and go back to region i. This process will repeat as long as the environment remains in state j. To address this issue, we assume $\bar{r}(t) = c$ whenever $\bar{X}(t) = iK$ and $Z(t) = j$ such that $j \in \mathcal{S}_i^+$ and $j \in \mathcal{S}_{i+1}^-$. This is justified because the effective input flow rate in this case is c (since $\bar{X}(t)$ is forced to remain at threshold iK). However, this leads to the distribution of $\{\bar{X}(t), t \geq 0\}$ having a mass at the threshold iK. Now, similar to (53), the dynamics of the energy flow in the considered system are described by

$$\frac{d\bar{X}(t)}{dt} = \begin{cases} \bar{r}(t) - c & \text{if } \bar{X}(t) > 0, \\ \max(\bar{r}(t) - c, 0) & \text{if } \bar{X}(t) = 0, \\ \min(\bar{r}(t) - c, 0) & \text{if } \bar{X}(t) = NK. \end{cases}$$

We will now develop an approach to compute the limiting availability of this system.

IV.6.1 Semi-Markov Process Model

In this subsection, we use a semi-Markov process (SMP) to model our system. Here we define the Markov regeneration epochs $\{S_n, n \geq 0\}$ as the times when the energy level in the system $\bar{X}(t)$ crosses a threshold (i.e. enters or leaves a region), or the environment changes from one state to another when the energy level is stuck at a threshold. This means that a Markov regeneration epoch can occur when one of these two possible events occur. Figure 16 shows instances of such Markov regeneration epochs in a sample path of $\bar{X}(t)$. We now define a random variable W_n which captures important information about the system at the Markov regeneration epoch S_n (assume $S_0 = 0$). We let $W_n = (i, j)$ if $\bar{X}(S_n) = iK$ and $Z(S_n) = j$. The state space of W_n is $\mathcal{T} := \{0, \ldots, N\} \times \mathcal{S}$. The first component of W_n tells us the threshold where the energy level is at time S_n. The second component of W_n tells us the state of the environment at S_n.

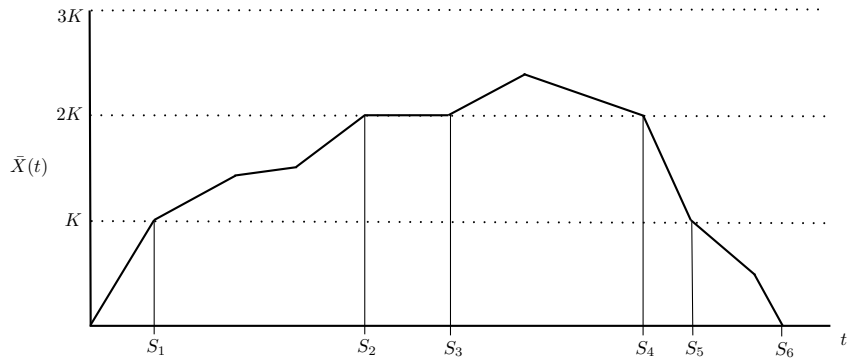

Figure 16: Markov regeneration epochs in a sample path of $\bar{X}(t)$

Theorem 6. *The sequence* $\{(W_n, S_n) : n \geq 0\}$ *is a Markov renewal sequence.*

Proof. Proof is similar to the proof of Theorem 3. □

Let $N(t) = \sup\{n \geq 0 : S_n \leq t\}$. Thus $N(t)$ is the number of Markov renewals in time t. Now we consider the process $\hat{W}(t) := W_{N(t)}$ for $t \geq 0$. Note that this process $\{\hat{W}(t), t \geq 0\}$ is a semi-Markov process (SMP) (Kulkarni [41]). We denote the kernel of this SMP as $\boldsymbol{G}(t) = [G_{(i,j)(k,l)}(t)]$, where $G_{(i,j)(k,l)}(t)$ is defined as

$$G_{(i,j)(k,l)}(t) = \mathrm{P}\{W_1 = (k,l), S_1 \leq t | W_0 = (i,j)\}, \qquad (i,j),(k,l) \in \mathcal{T}.$$

Note that $\{W_n, n \geq 0\}$ is an irreducible discrete-time Markov chain embedded in the SMP $\{\hat{W}(t), t \geq 0\}$. Given $W_n = (i,j)$, we can find out whether the energy level in the system is going to enter a region (which will be either region i or region $i+1$) after crossing the threshold iK or remain stuck at the threshold iK until the next regeneration epoch S_{n+1}. For example, if $W_n = (i,j)$ such that $0 < i < N$, $j \in \mathcal{S}_i^+$, and $j \in \mathcal{S}_{i+1}^+$, the energy level will increase and move into region $i+1$ after crossing the threshold iK. In another example, if $W_n = (i,j)$ such that $0 < i < N$, $j \in \mathcal{S}_i^+$, and $j \in \mathcal{S}_{i+1}^-$, the energy level is going to be stuck at the threshold iK until

the next regeneration epoch S_{n+1}. In all such cases where $W_n = (i, j)$ indicates that the energy level is going to to be stuck at the threshold iK, we call the state (i, j) a *sticky state*. The set of all sticky states is denoted by $\mathcal{T}_1$ and is given as

$$\mathcal{T}_1 = \{(i,j) \in \mathcal{T} : i = 0, j \in \mathcal{S}_1^-; \text{ or } i = N, j \in \mathcal{S}_N^+; \text{ or } 0 < i < N, j \in \mathcal{S}_i^+, j \in \mathcal{S}_{i+1}^-\}.$$

We will call the states in the set $\mathcal{T} \setminus \mathcal{T}_1$ as *non-sticky* states.

Let us now denote the transition probability matrix and stationary distribution of the embedded Markov chain $\{W_n, n \geq 0\}$ by $\hat{\boldsymbol{P}}$ and $\hat{\boldsymbol{\pi}}$ respectively. Also, let τ_{ij} be the expected sojourn time of the SMP $\{\hat{W}(t), t \geq 0\}$ in state (i, j) for $(i, j) \in \mathcal{T}$. Note that our system is considered to be unavailable when $\bar{X}(t) = 0$, i.e. when the energy level of the system is stuck at the threshold 0. Therefore the limiting availability of the system is precisely equal to the limiting probability that the SMP $\{\hat{W}(t), t \geq 0\}$ is not in a sticky state (i, j) such that $i = 0$ and $j \in \mathcal{S}_1^-$. By Theorem 9.27 in Kulkarni [41], we can compute the limiting availability of the system as

$$\bar{A} = \lim_{t\to\infty} \mathrm{P}\left(\hat{W}(t) \notin \{(0,j) : j \in \mathcal{S}_1^-\}\right) = 1 - \frac{\sum_{j\in\mathcal{S}_1^-} \hat{\pi}_{0j}\tau_{0j}}{\sum_{(i,j)\in\mathcal{T}} \hat{\pi}_{ij}\tau_{ij}}. \tag{70}$$

IV.6.2 Computation of Limiting Availability

To compute the limiting availability in (70), we need to find the stationary distribution $\hat{\boldsymbol{\pi}}$ of the Markov chain $\{W_n, n \geq 0\}$, and the mean sojourn times τ_{ij} of the SMP $\{\hat{W}(t), t \geq 0\}$. These quantities can be computed if the SMP kernel $\boldsymbol{G}(t)$ (or its LST $\tilde{\boldsymbol{G}}(w) = [\tilde{G}_{(i,j)(k,l)}(w)]$) is known. The expected sojourn times τ_{ij} can be computed as

$$\tau_{ij} = -\frac{d}{dw} \sum_{(k,l)} \widetilde{G}_{(i,j),(k,l)}(w) \quad \text{at } w = 0.$$

Further, note that the transition probability matrix of the Markov chain $\{W_n, n \geq 0\}$ is $\hat{\boldsymbol{P}} = \boldsymbol{G}(\infty) = \tilde{\boldsymbol{G}}(0)$. Therefore the stationary probabilities $\hat{\boldsymbol{\pi}}$ of this Markov chain can be found by solving the equations $\hat{\boldsymbol{\pi}} = \hat{\boldsymbol{\pi}}\tilde{\boldsymbol{G}}(0)$ and $\sum_{(i,j)\in\mathcal{T}} \hat{\pi}_{ij} = 1$.

Thus, to compute the limiting availability, we mainly need to find the kernel elements of the SMP $\{\hat{W}(t), t \geq 0\}$. In the following subsections, we provide approaches to compute the SMP kernel elements in LST form.

IV.6.2.1 Computing Kernel Elements for Sticky Initial States

Note that, when the SMP $\{\hat{W}(t), t \geq 0\}$ is in a sticky state $(i, j) \in \mathcal{T}_1$, the energy level of the system is stuck at the threshold iK for the entire sojourn time of the SMP in state (i, j). In this case, the SMP can only go to another state (k, l) such that $k = i$ and $l \neq j$. This change is only due to the change of state from j to l in the environment process which is described by a continuous time Markov chain with infinitesimal generator $\boldsymbol{Q} = [q_{ij}]$. Therefore, for $l \neq j$, we have in this case

$$G_{(i,j),(i,l)}(t) = \frac{q_{jl}}{-q_{jj}}\left(1 - e^{q_{jj}t}\right) \quad \text{and} \quad \tilde{G}_{(i,j),(i,l)}(w) = \frac{q_{jl}}{-q_{jj} + w}.$$

IV.6.2.2 Computing Kernel Elements for Non-sticky Initial States

Now we will show how to compute the remaining non-zero kernel elements that correspond to transition from a non-sticky state. Note that, if the SMP is in a non-sticky state, it means that energy level of the system is drifting through a region (which can be found by analyzing the non-sticky state). In this case, the SMP will change state when the energy level will hit either the top or bottom threshold of this region. For example, suppose the SMP is currently in a non-sticky state (i, j) such that $0 < i < N$, $j \in \mathcal{S}_i^-$, $j \in \mathcal{S}_{i+1}^-$. This means the energy level was at threshold iK at the beginning of this state and is currently in region i. The SMP will change to

state (i,l) when the energy level hits the upper threshold iK of this region, which will only happen if $l \in \mathcal{S}_i^+$. Similarly the SMP will change to state $(i-1,l)$ when the energy level hits the lower threshold $(i-1)K$ of this region, which will only happen if $l \in \mathcal{S}_i^-$. Thus the sojourn time of the SMP in a non-sticky state can be analyzed using first passage time analysis within a region, which we introduce next.

When the energy level is in region i, we define the first passage time to reach either the upper threshold iK or the lower threshold $(i-1)K$ as

$$T_i = \inf\left\{t \geq 0 : \bar{X}_i(t) = 0 \text{ or } \bar{X}_i(t) = K\right\},$$

where $\bar{X}_i(t) = \bar{X}(t) - (i-1)K$. Now consider the joint distribution

$$H_{jl}^i(x,t) = \mathrm{P}\{T_i \leq t, Z(T_i) = l | \bar{X}_i(0) = x, Z(0) = j\}$$

for $j,l \in \mathcal{S}$, $t \geq 0$, and $0 \leq x \leq K$. The distribution $\boldsymbol{H}^i(x,t) = [H_{jl}^i(x,t)]$ is known to satisfy the following partial differential equation.

$$\frac{\partial \boldsymbol{H}^i(x,t)}{\partial t} - \boldsymbol{D}^i \frac{\partial \boldsymbol{H}^i(x,t)}{\partial x} = \boldsymbol{Q}\boldsymbol{H}^i(x,t), \tag{71}$$

where $\boldsymbol{D}^i$ is a diagonal matrix with $[\boldsymbol{D}^i]_{jj} = (N-i+1)r_j - c$ for $j = 1,\ldots,|\mathcal{S}|$. The following boundary conditions hold for $H_{jl}^i(x,t)$.

$$\begin{aligned}
H_{jl}^i(K,t) &= 1 \qquad \text{if } j = l, j \in \mathcal{S}_i^+, \\
H_{jl}^i(K,t) &= 0 \qquad \text{if } j \neq l, j \in \mathcal{S}_i^+, \\
H_{jl}^i(0,t) &= 1 \qquad \text{if } j = l, j \in \mathcal{S}_i^-, \\
H_{jl}^i(0,t) &= 0 \qquad \text{if } j \neq l, j \in \mathcal{S}_i^-.
\end{aligned}$$

Taking the LST on both sides of (71) with respect to t, we obtain the following ordinary differential equation (ODE).

$$\boldsymbol{D}^i \frac{d\tilde{\boldsymbol{H}}^i(x,w)}{dx} = (w\boldsymbol{I} - \boldsymbol{Q})\tilde{\boldsymbol{H}}^i(x,w), \tag{72}$$

where $\tilde{\boldsymbol{H}}^i(x,t) = [\tilde{H}^i_{jl}(x,t)]$ and $\tilde{H}^i_{jl}(x,w) := \int_0^\infty e^{-wt}\ dH^i_{jl}(x,t)$. As in Section IV.4.1.1, we can solve the ODE (72) using spectral decomposition technique where the solution is of the same format as in (63).

Once $\tilde{\boldsymbol{H}}^i(x,w)$ is computed for every region i, we can construct the following non-zero kernel elements that correspond to transition from a non-sticky state.

$$\begin{aligned}
\tilde{G}_{(i,j),(i+1,l)}(w) &= \tilde{H}^{i+1}_{jl}(0,w) \quad \text{if } 0 \le i < N, j \in \mathcal{S}^+_{i+1}, l \in \mathcal{S}^+_{i+1}, \\
\tilde{G}_{(i,j),(i,l)}(w) &= \tilde{H}^{i+1}_{jl}(0,w) \quad \text{if } 0 \le i < N, j \in \mathcal{S}^+_{i+1}, l \in \mathcal{S}^-_{i+1}, \\
\tilde{G}_{(i,j),(i,l)}(w) &= \tilde{H}^{i}_{jl}(K,w) \quad \text{if } 0 < i \le N, j \in \mathcal{S}^-_{i}, l \in \mathcal{S}^+_{i}, \\
\tilde{G}_{(i,j),(i-1,l)}(w) &= \tilde{H}^{i}_{jl}(K,w) \quad \text{if } 0 < i \le N, j \in \mathcal{S}^-_{i}, l \in \mathcal{S}^-_{i}.
\end{aligned}$$

IV.6.3 Numerical Example

Consider a system of 3 sensor nodes (i.e. $N = 3$), each with energy storage capacity of $K = 50$. The environment is described by a continuous-time Markov chain with state space $\{1,2,3,4,5\}$ and infinitesimal generator matrix given by

$$\boldsymbol{Q} = \begin{bmatrix} -1 & 0.4 & 0.3 & 0.2 & 0.1 \\ 0.4 & -0.7 & 0.1 & 0.1 & 0.1 \\ 0.5 & 0.4 & -1.1 & 0.1 & 0.1 \\ 0.2 & 0.3 & 0.3 & -1 & 0.2 \\ 0.3 & 0.3 & 0.3 & 0.3 & -1.2 \end{bmatrix}.$$

The energy inflow rates in environment states 1 to 5 are given by the vector $\boldsymbol{r} = [1, 2, 3.5, 6, 11]$. The energy consumption rate of the sensor is $c = 9.9$. Now, based on our developed approach, we will compute a lower bound for the limiting availability of this multi-sensor system under an exhaustive service policy.

In this case, the sticky states are (0,1), (0,2), (1,3), (2,4) and (3,5). All other states in $\mathcal{T} = \{0, 1, 2, 3\} \times \{1, \ldots, 5\}$ are non-sticky states. Now, using our method described in Section IV.6.2, the stationary probabilities $\hat{\pi}_{ij}$ and expected sojourn times τ_{ij} are computed and are shown in Table 4. Using (70), the lower bound $\bar{A}_{\text{low}}$ for the limiting availability of the system is found to be

$$\bar{A}_{\text{low}} = 1 - \frac{\hat{\pi}_{01}\tau_{01} + \hat{\pi}_{02}\tau_{02}}{\sum_{(i,j)\in\mathcal{T}} \hat{\pi}_{ij}\tau_{ij}} = 0.8431.$$

We repeated our computations for different values of N. Table 5 shows the values of $\bar{A}_{\text{low}}$ for different N values. Observe that at most five sensors will be required to ensure that the system is nearly available at all times.

IV.7 Conclusion

In this chapter, we developed several analytical models to compute and analyze the limiting availability of energy harvesting sensor nodes. We introduced an approach to exactly compute the limiting availability of a single energy harvesting sensor node under a threshold-based activation policy. Since the rate of energy harvesting is very limited, it may not be possible to achieve a desired level of availability with only one sensor node. Hence we considered a multi-sensor system where it is sufficient to keep only one sensor ON at any time. However, for such a system, it is difficult to develop tractable methods to compute the system-level availability when the sensors in the system have finite energy storage capacity. Therefore, for this case, we developed an approach to compute an effective lower bound on the limiting

Table 4: Computed mean sojourn times and stationary probabilities ($N = 3$)

(i, j)	τ_{ij}	$\hat{\pi}_{ij}$
(0,1)	1.0000	0.2517
(0,2)	1.4286	0.2024
(0,3)	2.3999	0.1044
(0,4)	6.1231	0.0792
(0,5)	7.1305	0.0541
(1,1)	8.8536	0.0692
(1,2)	9.1410	0.0674
(1,3)	0.9091	0.0259
(1,4)	2.5019	0.0479
(1,5)	4.1502	0.0892
(2,1)	9.5557	0.0012
(2,2)	9.7492	0.0014
(2,3)	9.5873	0.0013
(2,4)	1.0000	0.0012
(2,5)	0.9977	0.0037
(3,1)	7.3603	1.8998×10^{-16}
(3,2)	7.3844	1.8998×10^{-16}
(3,3)	7.5500	1.8998×10^{-16}
(3,4)	7.8331	1.8998×10^{-16}
(3,5)	0.8333	7.5992×10^{-16}

Table 5: Computed availability lower bound

N	$\bar{A}_{\text{low}}$
1	0.1022
2	0.4487
3	0.8431
4	0.9914
5	$1 - 1.167 \times 10^{-5}$

availability of the system when an exhaustive service policy is used. Using this lower bound, we can have a good estimate of the number of sensors required to achieve a certain level of availability.

In our formulations for limiting availability, we used a Markov regenerative process model in case of a single sensor node and a semi-Markov process model (SMP) in case of the multi-sensor system. Note that an SMP based formulation can also be used in the single sensor node case. However, in this case, the Markov regenerative model is much simpler compared to the SMP model.

Many extensions of this work can be considered for future research. In our models, we have assumed that the discharge rate of the sensor is fixed at c. However, it will be worthwhile to consider certain application cases with a continuously changing discharge rate. We can extend our models to a case where the discharge process is similar to the recharge process and is modeled by another continuous-time Markov chain. In the cyclic exhaustive service policies considered in Section IV.5, we have ignored any switch-over time for making a transition from one sensor to another. However, when these switch-over times are significant, a different approach will be required to compute the limiting availability at the system level.

CHAPTER V

CONCLUSION

V.1 Research Summary and Contributions

In this dissertation, we developed efficient energy management policies for wireless sensor network applications where energy conservation adversely affects another crucial performance parameter. We studied the following energy-performance trade-off cases: energy and node replacement costs (Case I), energy and delay (Case II), and energy and availability (Case III). We considered these trade-off cases in three distinct problem cases. In each of these problem cases, we developed analytical formulations, and derived and/or analyzed policies that effectively manage the considered energy-performance trade-off. Our methods are based on approaches appropriate for the considered problems, and these include mixed-integer programming, Markov decision processes and stochastic fluid-flow analysis.

Overall this research makes new contributions to both operations research and communication networking literature. Specific to our considered problem cases, following are the main contributions of our work.

1. **Energy and node replacement cost model:** Our work is the first of its kind to consider the trade-off between energy and node replacement costs in a wireless sensor network application. Our solution idea involving joint control of routing and node replacement policies is also new. Though routing and node replacement problems have received a lot of attention in the literature, they have mostly been addressed independently. Based on our combined and routing and node replacement policy approach, we developed mathematical

formulations for minimizing the node replacement costs and derived effective policies suitable for practical implementation.

2. **Energy and delay model:** In this case, we developed a Markov decision process (MDP) based controller to make efficient "transmit or hold" decisions for packets at the relay node at every transmission opportunity. The structure of the MDP is uncommon, and the two-dimensional countable state space makes it quite challenging to solve for the optimal policy. We used certain convexity concepts in a novel way to derive structural properties of the optimal policy. We proved that, in a certain case, the optimal network coding policy for the relay node is a special kind of threshold policy. We also developed an analytical approach to compute the threshold policy. Moreover, we showed that some simple policies (e.g. see "transmit-all" and "rate-based" policies in Section III.6) can be as efficient as the threshold policy in particular situations. These policies are easy to implement, and there is no computational overhead when system parameters change. This makes these policies particularly attractive for practical implementation.

3. **Energy and availability model:** Availability of the sensor nodes is an important factor in the design and operation of energy harvesting sensor networks. Though the availability of various maintainable systems has been studied in the literature, there is very limited work on the availability of self-powered systems such as the energy harvesting sensor networks. We used stochastic fluid-flow analysis to develop methods to compute the limiting availability of energy harvesting sensor nodes for both finite and infinite energy capacity cases. We also developed a semi-Markov process based model to estimate the number of nodes required to achieve a desired level of availability.

V.2 Future Research

Specific to each of our considered problem cases, we have provided possible extensions of our work in Sections II.7, III.7, and IV.7 (for Cases I, II and III respectively). However, in the general area of this research, following directions can be explored in future.

1. **General network structure:** In our problem cases, we have considered wireless sensor network structures very specific to the nature of applications. For example, in Case I, we considered minimizing node replacement costs in a grid-structured wireless sensor network that is particularly suitable for seismic monitoring application. Also, in Case II, we considered network coding primarily in case of a single relay node and applied the policies derived in this case to a line network. Although we did not specifically consider the energy level of a node in this case, it would be an immediate extension. In Case III, we did not consider any network specific application. In all these cases, it is important to extend our models and formulations to a general network structure. Some of our considered problems will be intractable for a general network setting. In those cases, approximate solution procedures can be developed.

2. **Non-Markovian model:** In Case II, we assumed Poisson distributed packet arrival processes which led to the formulation our problem as a Markov decision process. Similarly, in Case III, we modeled the environment (which acts as the energy source) as a continuous-time Markov chain. In this case, we used the strong Markov property to derive important results that would have been hard to obtain in a non-Markovian energy flow model. However, in both Cases II and III, we can extend our models for general distributions (for the arrival processes) by approximating them as phase-type distributions.

3. **Other energy-performance trade-off issues:** We studied three important energy-performance trade-off situations in wireless sensor networks. However, depending on the nature of application of the sensor network, reducing energy consumption can affect many other performance parameters, e.g. network coverage, utilization, node-level fairness. Some these energy-performance trade-off issues are important, but have not been addressed adequately in the literature. These issues can be investigated.

REFERENCES

[1] V. Aggarwal, N. Gautam, S. R. T. Kumara, and M. Greaves. Stochastic fluid flow models for determining optimal switching thresholds. *Performance Evaluation*, 59(1):19–46, 2005.

[2] R. Ahlswede, N. Cai, S. R. Li, and R. W. Yeung. Network information flow. *IEEE Transactions on Information Theory*, 46(4):1204–1216, 2000.

[3] S. Ahn and V. Ramaswami. Efficient algorithms for transient analysis of stochastic fluid flow models. *Journal of Applied Probability*, 42(2):531–549, 2005.

[4] I. F. Akyildiz, D. Pompili, and T. Melodia. Underwater acoustic sensor networks: research challenges. *Ad Hoc Networks*, 3(3):257–279, 2005.

[5] I. F. Akyildiz, W. Su, Y. Sankarasubramaniam, and E. Cayirci. Wireless sensor networks: a survey. *Computer Networks*, 38(4):393–422, 2002.

[6] G. Anastasi, M. Conti, M. D. Francesco, and A. Passarella. Energy conservation in wireless sensor networks: A survey. *Ad Hoc Networks*, 7(3):537–568, 2009.

[7] D. Anick, D. Mitra, and M. M. Sondhi. Stochastic theory of a data handling system with multiple sources. *The Bell System Technical Journal*, 61:1871–1894, 1982.

[8] A. Arapostathis, V. S. Borkar, E. Fernández-Gaucherand, M. K. Ghosh, and S. I. Marcus. Discrete-time controlled markov processes with average cost criterion: a survey. *SIAM Journal on Control and Optimization*, 31(2):282–344, 1993.

[9] D. Assaf and J. G. Shanthikumar. Optimal group maintenance policies with continuous and periodic inspections. *Management Science*, 33(11):1440–1452, 1987.

[10] J. W. Baek, H. W. Lee, S. W. Lee, and S. Ahn. A markov-modulated fluid flow queueing model under d-policy. *Numerical Linear Algebra with Applications*, 18(6):993–1010, 2011.

[11] N. Barbot, B. Sericola, and M. Telek. Distribution of busy period in stochastic fluid models. *Stochastic Models*, 17(4):407–427, 2001.

[12] V. S. Borkar. Control of markov chains with long-run average cost criterion: The dynamic programming equations. *SIAM Journal on Control and Optimization*, 27(3):642–657, 1989.

[13] L. Brekhovskikh and Y. Lysanov. *Fundamentals of Ocean Acoustics*. Springer, New York, 1982.

[14] R. Cavazos-Cadena. Necessary conditions for the optimality equation in average-reward markov decision processes. *Applied Mathematics and Optimization*, 19(1):97–112, 1989.

[15] R. Cavazos-Cadena and L. I. Sennott. Comparing recent assumptions for the existence of average optimal stationary policies. *Operations Research Letters*, 11(1):33–37, 1992.

[16] J.-H. Chang and L. Tassiulas. Maximum lifetime routing in wireless sensor networks. *IEEE/ACM Transactions on Networking*, 12(4):609–619, 2004.

[17] E. Ciftcioglu, Y. Sagduyu, R. Berry, and A. Yener. Cost-delay tradeoffs for two-way relay networks. *IEEE Transactions on Wireless Communications*, 10(12):4100–4109, 2011.

[18] R. Dekker and I. F. Roelvink. Marginal cost criteria for preventive replacement of a group of components. *European Journal of Operational Research*, 84(2):467–480, 1995.

[19] P. M. Duncan. Is there a future for passive seismic? *First Break*, 23(6):111–115, 2005.

[20] M. Effros, T. Ho, and S. Kim. A tiling approach to network code design for wireless networks. In *Proceedings of the IEEE Information Theory Workshop (ITW)*, pages 62–66, 2006.

[21] A. Es-Saghouani and M. Mandjes. Transient analysis of markov-fluid-driven queues. *Top*, 19(1):35–53, 2011.

[22] N. Gautam. *Analysis of Queues: Methods and Applications*. CRC Press, Boca Raton, FL, 2012.

[23] X. He and A. Yener. On the energy-delay trade-off of a two-way relay network. In *Proceedings of the 42nd Annual Conference on Information Sciences and Systems (CISS)*, pages 865–870, 2008.

[24] J. Heidemann, W. Ye, J. Wills, A. Syed, and Y. Li. Research challenges and applications for underwater sensor networking. In *Proceedings of the IEEE Wireless Communications and Networking Conference (WCNC)*, pages 228–235, 2006.

[25] B. Heidergott. A weak derivative approach to optimization of threshold parameters in a multicomponent maintenance system. *Journal of Applied Probability*, 38(2):386–406, 2001.

[26] B. Heidergott and T. Farenhorst-Yuan. Gradient estimation for multicomponent maintenance systems with age-replacement policy. *Operations Research*, 58(3):706–718, 2010.

[27] W. R. Heinzelman, A. Chandrakasan, and H. Balakrishnan. Energy-efficient communication protocol for wireless microsensor networks. In *Proceedings of*

the 33rd Hawaii International Conference on System Sciences (HICSS), pages 1–10, 2000.

[28] Y.-P. Hsu, N. Abedini, S. Ramasamy, N. Gautam, A. Sprintson, and S. Shakkottai. Opportunities for network coding: To wait or not to wait. In *Proceedings of the IEEE International Symposium on Information Theory (ISIT)*, pages 791–795, 2011.

[29] N. Jaggi, K. Kar, and A. Krishnamurthy. Near-optimal activation policies in rechargeable sensor networks under spatial correlations. *ACM Transactions on Sensor Networks*, 4(3):17:1–17:36, 2008.

[30] G. Jones, P. Harrison, U. Harder, and T. Field. Fluid queue models of battery life. In *Proceedings of the 19th IEEE International Symposium on Modeling, Analysis and Simulation of Computer and Telecommunication Systems (MASCOTS)*, pages 278–285, 2011.

[31] K. Kalpakis, K. Dasgupta, and P. Namjoshi. Efficient algorithms for maximum lifetime data gathering and aggregation in wireless sensor networks. *Computer Networks*, 42(6):697–716, 2003.

[32] A. Kansal, J. Hsu, S. Zahedi, and M. B. Srivastava. Power management in energy harvesting sensor networks. *ACM Transactions in Embedded Computing Systems*, 6(4):32:1–32:38, 2007.

[33] A. Kansal and M. B. Srivastava. An environmental energy harvesting framework for sensor networks. In *Proceedings of the International Symposium on Low Power Electronics and Design (ISLPED)*, pages 481–486, 2003.

[34] K. Kar, A. Krishnamurthy, and N. Jaggi. Dynamic node activation in networks of rechargeable sensors. *IEEE/ACM Transactions on Networking*, 14(1):15–26,

2006.

[35] S. Katti, H. Rahul, W. Hu, D. Katabi, M. Médard, and J. Crowcroft. Xors in the air: practical wireless network coding. *ACM SIGCOMM Computer Communication Review*, 36(4):243–254, 2006.

[36] J. Kharoufeh, D. Finkelstein, and D. Mixon. Availability of periodically inspected systems with markovian wear and shocks. *Journal of Applied Probability*, 43(2):303–317, 2006.

[37] J. P. Kharoufeh and N. Gautam. Deriving link travel-time distributions via stochastic speed processes. *Transportation Science*, 38(1):97–106, 2004.

[38] P. Kiessler, G. Klutke, and Y. Yang. Availability of periodically inspected systems subject to markovian degradation. *Journal of Applied Probability*, 39(4):700–711, 2002.

[39] D. Kilfoyle and A. Baggeroer. The state of the art in underwater acoustic telemetry. *IEEE Journal of Oceanic Engineering*, 25(1):4–27, 2000.

[40] K. A. H. Kobbacy, D. N. P. Murthy, R. P. Nicolai, and R. Dekker. Optimal maintenance of multi-component systems: A review. In *Complex System Maintenance Handbook*, pages 263–286. Springer, London, 2008.

[41] V. G. Kulkarni. *Modeling and analysis of stochastic systems.* Chapman & Hall/CRC, Boca Raton, FL, 1995.

[42] V. G. Kulkarni. Fluid models for single buffer systems. In *Frontiers in Queueing: Models and Applications in Science and Engineering*, pages 321–338. CRC Press, Boca Raton, FL, 1997.

[43] V. G. Kulkarni and E. Tzenova. Mean first passage times in fluid queues. *Operations Research Letters*, 30(5):308–318, 2002.

[44] L. Lanbo, Z. Shengli, and C. Jun-Hong. Prospects and problems of wireless communication for underwater sensor networks. *Wireless Communications and Mobile Computing*, 8(8):977–994, 2008.

[45] P. L'Ecuyer, B. Martin, and F. J. Vázquez-Abad. Functional estimation for a multicomponent age replacement model. *American Journal of Mathematical and Management Sciences*, 19(1-2):135–156, 1999.

[46] Y. Li, W. Ye, J. Heidemann, and R. Kulkarni. Design and evaluation of network reconfiguration protocols for mostly-off sensor networks. *Ad Hoc Networks*, 6(8):1301–1315, 2008.

[47] L. Lin, N. B. Shroff, and R. Srikant. Asymptotically optimal energy-aware routing for multihop wireless networks with renewable energy sources. *IEEE/ACM Transactions on Networking*, 15(5):1021–1034, 2007.

[48] S. R. Mahabhashyam, N. Gautam, and S. R. T. Kumara. Resource-sharing queueing systems with fluid-flow traffic. *Operations Research*, 56(3):728–744, 2008.

[49] N. Martakis, S. Kapotas, and G. Tselentis. Integrated passive seismic acquisition and methodology. case studies. *Geophysical Prospecting*, 54(6):829–847, 2006.

[50] S. C. Maxwell and T. I. Urbancic. The role of passive microseismic monitoring in the instrumented oil field. *The Leading Edge*, 20(6):636–639, 2001.

[51] M. Médard and A. Sprintson. *Network coding: Fundamentals and applications*. Academic Press, Waltham, MA, 2011.

[52] K. Murota. Recent developments in discrete convex analysis. In *Research Trends in Combinatorial Optimization*, pages 219–260. Springer-Verlag, Berlin Heidelberg, 2009.

[53] A. Narayanan and V. G. Kulkarni. First passage times in fluid models with an application to two priority fluid systems. In *Proceedings of the 2nd International Computer Performance and Dependability Symposium (IPDS)*, pages 166–175, 1996.

[54] S. Parikh, V. Vokkarane, L. Xing, and D. Kasilingam. Node-replacement policies to maintain threshold-coverage in wireless sensor networks. In *Proceedings of the 16th International Conference on Computer Communications and Networks (ICCCN)*, pages 760–765, 2007.

[55] D. Pompili and T. Melodia. Three-dimensional routing in underwater acoustic sensor networks. In *Proceedings of the 2nd ACM International Workshop on Performance Evaluation of Wireless Ad-hoc, Sensor, and Ubiquitous Networks (PE-WASUN)*, pages 214–221, 2005.

[56] M. Puterman. *Markov decision processes: Discrete stochastic dynamic programming*. Wiley-Interscience, New York, 2005.

[57] V. Raghunathan, S. Ganeriwal, and M. B. Srivastava. Emerging techniques for long lived wireless sensor networks. *IEEE Communications Magazine*, 44(4):108–114, 2006.

[58] S. Resnick. *Adventures in stochastic processes*. Birkhäuser, Boston, 1992.

[59] P. Ritchken and J. G. Wilson. (m, t) group maintenance policies. *Management Science*, 36(5):632–639, 1990.

[60] M. Schäl. Average optimality in dynamic programming with general state space. *Mathematics of Operations Research*, 18(1):163–172, 1993.

[61] SeaBed Geophysical. Practical applications for node seismic. *First Break*, 25(12):89–92, 2007.

[62] L. I. Sennott. A new condition for the existence of optimal stationary policies in average cost markov decision processes. *Operations Research Letters*, 5(1):17–23, 1986.

[63] L. I. Sennott. Average cost optimal stationary policies in infinite state markov decision processes with unbounded costs. *Operations Research*, 37(4):626–633, 1989.

[64] L. I. Sennott. The average cost optimality equation and critical number policies. *Probability in the Engineering and Informational Sciences*, 7(1):47–67, 1993.

[65] L. I. Sennott. *Stochastic Dynamic Programming and the Control of Queueing Systems*. Wiley-Interscience, New York, 1999.

[66] R. Seymour and F. Barr. An improved seabed seismic 4d data collection method for reservoir monitoring. In *Proceedings of the European Petroleum Conference*, pages 189–194, 1996.

[67] R. C. Shah and J. M. Rabaey. Energy aware routing for low energy ad hoc sensor networks. In *Proceedings of IEEE Wireless Communications and Networking Conference (WCNC)*, pages 350–355, 2002.

[68] V. Sharma, U. Mukherji, V. Joseph, and S. Gupta. Optimal energy management policies for energy harvesting sensor nodes. *IEEE Transactions on Wireless Communications*, 9(4):1326–1336, 2010.

[69] S. Singh, M. Woo, and C. S. Raghavendra. Power-aware routing in mobile ad hoc networks. In *Proceedings of the 4th ACM/IEEE International Conference on Mobile Computing and Networking (MobiCom)*, pages 181–190, 1998.

[70] J. Skellam. The frequency distribution of the difference between two poisson variates belonging to different populations. *Journal of the Royal Statistical*

Society, 109(3):296–296, 1946.

[71] R. Srivastava and C. E. Koksal. Basic tradeoffs for energy management in rechargeable sensor networks. `http://arxiv.org/abs/1009.0569`.

[72] M. Stojanovic. On the relationship between capacity and distance in an underwater acoustic communication channel. In *Proceedings of the 1st ACM International Workshop on Underwater Networks (WUWNet)*, pages 41–47, 2006.

[73] H. Takagi. Queuing analysis of polling models. *ACM Computing Surveys (CSUR)*, 20(1):5–28, 1988.

[74] B. Tong, G. Wang, W. Zhang, and C. Wang. Node reclamation and replacement for long-lived sensor networks. In *Proceedings of the 6th IEEE Communications Society Conference on Sensor, Mesh and Ad-hoc Communications and Networks (SECON)*, pages 1–9, 2009.

[75] R. J. Urick. *Principles of underwater sound*. McGraw-Hill, New York, 1983.

[76] I. Vasilescu, K. Kotay, D. Rus, M. Dunbabin, and P. Corke. Data collection, storage, and retrieval with an underwater sensor network. In *Proceedings of the 3rd International Conference on Embedded Networked Sensor Systems (SenSys)*, pages 154–165, 2005.

[77] J. G. Wilson and A. Benmerzouga. Bayesian group replacement policies. *Operations Research*, 43(3):471–476, 1995.

[78] L. A. Wolsey. *Integer Programming*. Wiley-Interscience, New York, 1998.

[79] J. Yick, B. Mukherjee, and D. Ghosal. Wireless sensor network survey. *Computer Networks*, 52(12):2292–2330, 2008.

[80] K. Zeng, K. Ren, W. Lou, and P. J. Moran. Energy aware efficient geographic routing in lossy wireless sensor networks with environmental energy supply. *Wireless Networks*, 15(1):39–51, 2009.

[81] X. Zheng. All opportunity-triggered replacement policy for multiple-unit systems. *IEEE Transactions on Reliability,*, 44(4):648–652, 1995.

APPENDIX A

EXPRESSION FOR $P_T(f, d)$

In this appendix, we use some of the available results to develop a mathematical expression for $P_T(f, d)$ (see Section II.4) which is the power required by an acoustic transmitter to transmit upto a distance d at frequency f. We use this expression in (17) to compute the energy consumption in wireless acoustic transmission.

The passive sonar equation describing major energy losses (given by signal-to-noise ratio SNR) in an acoustic transmission is given as (Urick [75]):

$$SNR = SL - TL - NL + DI, \tag{73}$$

where SL is the source level, TL is the transmission loss, NL is the noise level and DI is the directivity index. All quantities in (73) are in dB re μPa, where the reference pressure of 1 μPa corresponds to the reference intensity 0.67×10^{-18} W/m^2. Assuming ambient noise level NL of 70 dB, a target SNR of 20 dB at the receiver and not considering directivity effect, we will have a required source level $SL = TL + 90$ dB.

The transmission loss TL has a highly non-linear relationship with distance and frequency. Its expression involving major path loss components is given as (Urick [75]):

$$TL = 10 \log d^2 + d \times 10^{-3} \times 10 \log \alpha(f), \tag{74}$$

where the first term in the summation represents spreading loss and the second term represents absorption loss. These losses are explained in greater detail in the works by Lanbo *et al.* [44], Stojanovic [72] and Urick [75]. We have assumed spherical

spreading considering that the nodes are mounted at deep underwater locations. In fact this spreading factor in practice would be tuned based on measurements. In (74), $\alpha(f)$ is the absorption coefficient, and it is expressed in dB/km for frequency f [kHz] by Thorp's formula as (Brekhovskikh and Lysanov [13]):

$$10\log\alpha(f) = 0.11\frac{f^2}{1+f^2} + 44\frac{f^2}{4100+f^2} + 2.75\times10^{-4}f^2 + 0.003.$$

Now we will use the estimate of $SL = TL + 90$ to find an expression for the required transmission power $P_T(f,d)$. The source level SL is defined as the intensity I at a reference point located at a distance of 0.9144 m (which is equal to 1 yard) from the acoustic center of the source, relative to the reference intensity $I_{\text{ref}} = 0.67\times10^{-18}$ W/m^2 in underwater acoustics (Urick [75]).

$$SL = 10\log\frac{I}{I_{\text{ref}}}.$$

If SL is targeted to achieve the required SNR at a distance d, the transmitter power required to produce the intensity I at the reference point is also the minimum power required to transmit up to distance d. Hence, for a given frequency f, we can find the transmitter power [W] as

$$P_T(f,d) = 0.67\times10^{-18}\times4\pi(0.9144)^2\times10^{\frac{(10\log d^2 + d\times10^{-3}\times10\log\alpha(f))+90}{10}}.$$